Computer Modeling in Engineering & Sciences

Tech Science Press

Doi:10.32604/cmes.2025.058362

ARTICLE

A Heavy Tailed Model Based on Power XLindley Distribution with Actuarial Data Applications

Mohammed Elgarhy[1], **Amal S. Hassan**[2], **Najwan Alsadat**[3], **Oluwafemi Samson Balogun**[4], **Ahmed W. Shawki**[5] **and Ibrahim E. Ragab**[6,*]

[1]Department of Basic Sciences, Higher Institute of Administrative Sciences, Belbeis, 44621, Egypt
[2]Faculty of Graduate Studies for Statistical Research, Cairo University, Giza, 12613, Egypt
[3]Department of Quantitative Analysis, College of Business Administration, King Saud University, Riyadh, 11587, Saudi Arabia
[4]Department of Computing, University of Eastern Finland, Joensuu, 80130, Finland
[5]Central Agency for Public Mobilization & Statistics (CAPMAS), Cairo, 11819, Egypt
[6]Department of Basic Sciences, Egyptian Institute of Alexandria Academy for Management and Accounting, EIA, Alexandria, 21919, Egypt

*Corresponding Author: Ibrahim E. Ragab. Email: ibrahim.ragab@eia.edu.eg

Received: 10 September 2024; Accepted: 08 February 2025; Published: 03 March 2025

ABSTRACT: Accurately modeling heavy-tailed data is critical across applied sciences, particularly in finance, medicine, and actuarial analysis. This work presents the heavy-tailed power XLindley distribution (HTPXLD), a unique heavy-tailed distribution. Adding one more parameter to the power XLindley distribution improves this new distribution, especially when modeling leptokurtic lifetime data. The suggested density provides greater flexibility with asymmetric forms and different degrees of peakedness. Its statistical features, like the quantile function, moments, extropy measures, incomplete moments, stochastic ordering, and stress-strength parameters, are explored. We further investigate its use in actuarial science through the computation of pertinent metrics, such as value-at-risk, tail value-at-risk, tail variance, and tail variance premium. To obtain the point and interval parameter estimates, we use the maximum likelihood estimation approach. We do many simulation tests to evaluate the performance of our proposed estimator. Metrics like bias, relative bias, mean squared error, root mean squared error, average interval length, and coverage probability will be used in these tests to assess the estimator's performance. To illustrate the practical value of our proposed model, we apply it to analyze three real-world datasets. We then compare its performance to established competing models, highlighting its advantages.

KEYWORDS: Power XLindley; heavy-tailed-G family; extropy measure; stochastic ordering; parametric estimation; asymmetric dataset

1 Introduction

An essential area of statistics is lifetime data analysis, which models and examines the duration until a phenomenon fails or survives. It is useful in a wide range of disciplines, including biology, ecology, medicine, social sciences, and reliability engineering. The exponential distribution, with its constant failure rate function and memoryless quality, is one of the most popular distributions for lifespan data. Nevertheless, certain data types, such as those that show growing, declining, unimodal, or bathtub-shaped failure rate functions, might not be well-modeled by the exponential distribution. To get around the drawbacks of the exponential distribution and offer improved flexibility, many alternative distributions have been put forth in the literature. In this sense, one of the most flexible and straightforward lifespan models is the XLindley distribution (XLD), which was introduced by Chouia et al. [1] as a combination of the Lindley and the exponential distributions. The probability density function (PDF) and cumulative distribution function (CDF) of the XLD are defined as:

$$f(x;\beta) = \left(\frac{\beta^2(2+\beta+x)}{(1+\beta)^2}\right)e^{-\beta x}; \quad x > 0,$$

and

$$F(x;\beta) = 1 - \left(1 + \frac{\beta x}{(1+\beta)^2}\right)e^{-\beta x}; \quad x > 0,$$

where $\beta > 0$ is the scale parameter. Many academics have recently proposed various methods for incorporating new probability distributions. A strategy that increases the flexibility of the resulting distribution is the power transformation of the research variable with an additional shape parameter such as the power half-logistic distribution [2], power length-biased Suja distribution [3], power Lindley-G family [4], power weighted Sujayha distribution [5], power Lomax distribution [6], power Lomax Poisson distribution [7], power-modified Kies-exponential distribution [8], and power-transmuted inverse Rayleigh distribution [9]. In contrast to XLD, the power XLD (PXLD) produced by Meriem et al. [10] has an additional shape parameter that we will be focusing on here. The PDF and CDF of the PXLD are provided as below:

$$f(y;\vartheta,\beta) = \left(\frac{\vartheta\beta^2(2+\beta+y^{\vartheta})y^{\vartheta-1}}{(1+\beta)^2}\right)e^{-\beta y^{\vartheta}}; \quad y > 0, \tag{1}$$

and

$$F(y;\vartheta,\beta) = 1 - \left(1 + \frac{\beta y^{\vartheta}}{(1+\beta)^2}\right)e^{-\beta y^{\vartheta}}; \quad y > 0, \tag{2}$$

where $\beta > 0$ and $\vartheta > 0$ are scale and shape parameters, respectively.

In numerous fields of study during the past decades, including economics, actuarial science, engineering, environmental research, lifespan, medical science, and many more, it has been determined that the classical distributions do not match the data well. To construct many unique models tailored for certain datasets, the authors have gone into great detail in their explanation. The classical distributions may be made more flexible by introducing additional parameters or by performing various transformations on the baseline distribution, which will improve its capacity to handle complex situations. To strengthen the flexibility of models in this context, many classes of distributions have been generated by using various processes, resulting in a more powerful and adaptable distribution for dataset modeling; for instance, Marshall-Olkin-G [11], beta-G [12], Kumaraswamy-G [13], transformed-transformer [14], Weibull-G [15], Dinesh-Umesh-Sanjay-G by [16], type I half-logistic-G [17], exponentiated half-logistic-G [18], Topp-Leone-G [19], Gompertz-G [20], beta odd Lindley-G [21], truncated power Lomax-G [22], Kavya-Manoharan-G [23], odd inverted Topp-Leone [24], Weibull Marshall-Olkin-G [25], sec-G [26], length-biased truncated Lomax-G [27], generalized logarithmic-X [28], alpha log power transformed-G [29], Marshall-Olkin-exponentiated half logistic-G [30] among others.

Probability distributions with a significant number of values in the tail of the distribution that is more than what would be predicted from a normal distribution are referred to as heavy-tailed (HT) distributions. This means that HT distributions assign a higher probability to extreme events or outliers. These distributions are valuable tools in various fields for understanding and managing the risk associated with rare but impactful events. The necessity of the HT distributions in actuarial practice has prompted actuaries to develop new flexible distributions (see [31–33]). Reference [34] covered the characteristics, estimates, and fundamental ideas of HT distributions, whereas reference [35] examined the estimation issue of HT distributions in extreme value theory. Moreover, several specific HT distributions have been introduced, including the HT Gleser distribution by [36], Type-I HT-G distributions by [37], Type I HT odd power generalized Weibull-G by [38], and HT generalized Topp-Leone-G by [39]. Many actual application studies in a variety of fields, including hydrology, biology, agriculture, production, survival, and finance, may be shown using the HT class of distributions. In recent times, Ahmed et al. [40] have introduced a new class of distributions dubbed the HT class of distributions. To better examine the underlying patterns of the data sets, this new addition is a useful tool for creating new models that are suitable for analyzing HT, symmetric, complicated, and skewed data sets. The HT-G family of distributions' CDF and PDF may be written as follows, in that order:

$$G(y;\delta;\upsilon)=\frac{\delta F(y;\upsilon)}{\delta-1+F(y;\upsilon)},\quad \delta>1,\, y\in R, \tag{3}$$

and

$$g(y;\delta;\upsilon)=\frac{\delta(\delta-1)f(y;\upsilon)}{[\delta-1+F(y;\upsilon)]^2},\quad \delta>1,\, y\in R, \tag{4}$$

where $F(y;\upsilon)$, and $f(y;\upsilon)$ are the CDF and PDF of the baseline random variable with vector parameter υ.

The field of statistics has a large collection of probability distributions, each with its strengths and weaknesses. It is not possible to represent or express important aspects in every scenario using a single distribution. In response to this limitation, we introduce a novel extension of the PXLD with the assistance of the HT-G family, named the heavy-tailed PXLD (HTPXLD). This paper aims to achieve the following objectives:

- Create a flexible distribution that can display declining, right-skewed, and unimodal data. Its hazard rate function (HRF) can be growing, decreasing, unimodal, right-skewed, or reverse J-shaped.
- To construct and evaluate some of the key mathematical properties, including moments, linear representation of density function, incomplete moments (IMs), quantile function (QF), Bonferroni and Lorenz curves, stochastic ordering (SO), extropy measures, and stress-strength (SS) reliability parameter.
- To obtain the point and approximate confidence interval (CI) estimators of the unknown parameters of the HTPXLD using the maximum likelihood (ML) estimation method. Through the implementation of the Monte Carlo simulation approach, the accuracy of the proposed model estimates is evaluated.
- A comparative analysis of the proposed model against well-known alternatives is performed using three diverse real-world datasets to assess its practical applicability.

The paper proceeds as follows: Section 2 introduces the HTPXLD. Section 3 delves into its mathematical features. Few actuarial measures are examined in Section 4. In Section 5, we describe the process of estimating model parameters using the ML approach and create CIs for the unknown parameters of the model. A Monte Carlo simulation study is performed in Section 6 to demonstrate the consistency of the suggested estimate. Practical applications of the model are presented in Section 7. Section 8 concludes the paper with some final considerations and key findings.

2 Heavy-Tailed Power XLindley Distribution

This section introduces the core concepts behind the HTPXLD, including PDF, CDF, survival function (SF), HRF, and reversed HRF (RHRF). It also provides visualizations for the PDF and HRF. The CDF of the

HTPXLD is created by inserting CDF (2) in CDF (3), resulting in the following expression:

$$G(y;\omega) = \frac{\delta\left[1-\left(1+\beta^{\bullet} y^{\vartheta}\right) e^{-\beta y^{\vartheta}}\right]}{\delta-\left(1+\beta^{\bullet} y^{\vartheta}\right) e^{-\beta y^{\vartheta}}}, \quad y;>0, \beta, \vartheta>0, \delta>1, \tag{5}$$

where $\beta^{\bullet} = \frac{\beta}{(1+\beta)^2}$, $\omega = (\delta, \beta, \vartheta)$ is the set of parameters. The PDF of the HTPXLD is given by

$$g(y;\omega) = \frac{\delta(\delta-1)\beta^{\bullet}\vartheta\beta(2+\beta+y^{\vartheta})y^{\vartheta-1}e^{-\beta y^{\vartheta}}}{\left[\delta-\left(1+\beta^{\bullet} y^{\vartheta}\right) e^{-\beta y^{\vartheta}}\right]^2}, y>0, \delta>1, \vartheta, \beta>0. \tag{6}$$

For $\vartheta = 1$, the PDF (6) reduces to the HT XLD (HTXLD) as a special new sub-model. A key idea in survival analysis, reliability engineering, and other domains is the SF, sometimes referred to as the reliability function. It gives the probability that a system or component will operate perfectly for a predetermined amount of time. The SF of the HTXLD is given by

$$\bar{G}(y;\omega) = \frac{(\delta-1)\left(1+\beta^{\bullet} y^{\vartheta}\right) e^{-\beta y^{\vartheta}}}{\delta-\left(1+\beta^{\bullet} y^{\vartheta}\right) e^{-\beta y^{\vartheta}}}.$$

A mathematical notion utilized in survival analysis, reliability engineering, and other domains is the HRF, represented by $h(y;\omega)$. It measures the immediate risk of failure for a system or object that has so far survived at a given time (y). The HRF of the HTXLD is given by

$$h(y;\omega) = \frac{\delta\beta^{\bullet}\vartheta\beta(2+\beta+y^{\vartheta})y^{\vartheta-1}}{\left(1+\beta^{\bullet} y^{\vartheta}\right)\left[\delta-\left(1+\beta^{\bullet} y^{\vartheta}\right) e^{-\beta y^{\vartheta}}\right]}.$$

The RHRF of the HTXLD is given by

$$\bar{h}(y;\omega) = \frac{(\delta-1)\beta^{\bullet}\vartheta\beta(2+\beta+y^{\vartheta})y^{\vartheta-1}e^{-\beta y^{\vartheta}}}{\left[1-(1+\beta^{\bullet} y^{\vartheta})e^{-\beta y^{\vartheta}}\right]\left[\delta-\left(1+\beta^{\bullet} y^{\vartheta}\right) e^{-\beta y^{\vartheta}}\right]}.$$

The PDF plots of the HTPXLD for particular parameter values are shown in Fig. 1. The HRF of the HTPXLD for the chosen parameter values is then shown in Fig. 2. From Figs. 1 and 2, we can note that the PDF can be right-skewed, unimodal, or decreasing, but the HRF can be increasing, decreasing, or upside-down.

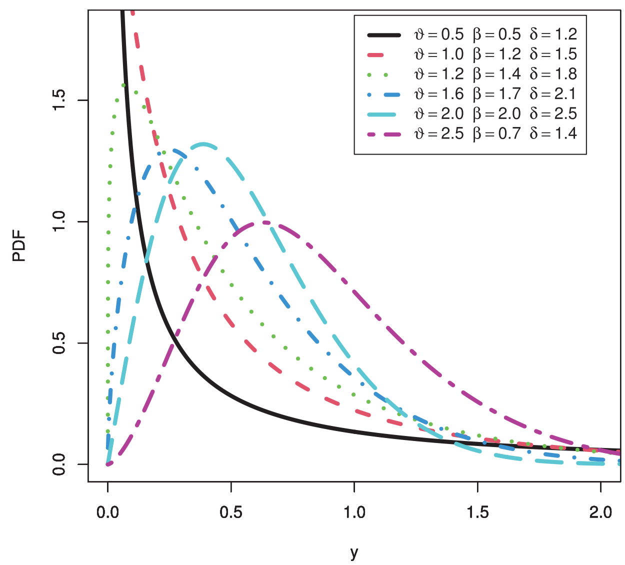

Figure 1: Plots of the PDF for the HTPXLD

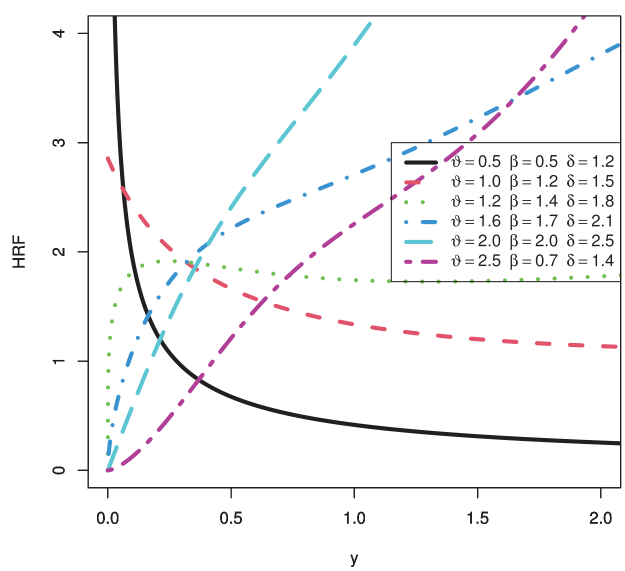

Figure 2: Plots of the HRF for the HTPXLD

3 Statistical Properties

A number of statistical properties, such as QF, moments, IMs, PDF linear expansion, Bonferroni and Lorenz curves, SO, SS parameters, and extropy measures that shed light on the structure of the distribution, will be covered here.

3.1 Series Representation

To analyze most of the statistical properties of HTPXLD, we can express the PDF as a linear combination of simpler functions. Using the following power series:

$$(1+z)^{-n} = \sum_{j_1=0}^{\infty} (-1)^{j_1} \binom{n+j_1-1}{j_1} z^{j_1}, \quad |z|<1, \quad n>0, \tag{7}$$

in PDF defined in Eq. (6) provides

$$f(y;\omega) = \sum_{j_1=0}^{\infty} \frac{(j_1+1)(-1)^{j_1}(\delta-1)\beta^{\bullet}\vartheta\beta}{\delta^{j_1+1}} \left(1+\beta^{\bullet}y^{\vartheta}\right)^{j_1} \left(2+\beta+y^{\vartheta}\right) y^{\vartheta-1} e^{-\beta(j_1+1)y^{\vartheta}}. \tag{8}$$

Again, using a binomial expansion in PDF (8) yields

$$\left.\begin{aligned} f(y;\omega) &= \sum_{j_1=0}^{\infty} \tau_{j_1,j_2}\vartheta\left(2+\beta+y^{\vartheta}\right) y^{\vartheta(j_2+1)-1} e^{-\beta(j_1+1)y^{\vartheta}} \\ \tau_{j_1,j_2} &= \sum_{j_2=0}^{j_1} \binom{j_1}{j_2} \frac{(j_1+1)(-1)^{j_1}(\delta-1)\beta^{\bullet(j_2+1)}\beta}{\delta^{j_1+1}} \end{aligned}\right\}. \tag{9}$$

3.2 Quantile Function

In statistical modeling, the QF is essential because it makes it possible to estimate certain percentiles, offers valuable insights into the data distribution, and supports a range of inferential and decision-making procedures. One may determine the QF of the HTPXLD, denoted as $Q(u)$, by solving $F(Q(u)) = u$ for $u \in (0,1)$. Therefore, we must create the following equation:

$$u = \frac{\delta\left[1-\left(1+\beta^{\bullet}(Q(u))^{\vartheta}\right)e^{-\beta(Q(u))^{\vartheta}}\right]}{\delta-\left(1+\beta^{\bullet}(Q(u))^{\vartheta}\right)e^{-\beta(Q(u))^{\vartheta}}},$$

which leads to

$$\frac{u\delta-\delta}{u-\delta} = \left(1+\beta^{\bullet}(Q(u))^{\vartheta}\right)e^{-\beta(Q(u))^{\vartheta}}. \tag{10}$$

By multiplying the two sides of Eq. (10) by $e^{-(\beta+1)^2}$, one may find the Lambert equation (see [41]), which gives

$$Q(u) = \left[-\frac{(\beta+1)^2}{\beta} - \frac{1}{\beta}\, W_{-1}\left\{\left(\frac{u\delta-\delta}{u-\delta}\right)(\beta+1)^2 e^{-(\beta+1)^2}\right\}\right]^{1/\vartheta}, \quad u \in (0,1). \tag{11}$$

Setting u to be equal $0.25, 0.5$, and 0.75 in Eq. (11) yields the first (Q_1), second (Q_2), and third (Q_3) quartiles of the HTPXLD. These quartiles help assess the symmetry (skewness) and peakedness (kurtosis) of the data. Bowley's skewness (η_1) ([42]) and Moor's kurtosis (η_2) ([43]) are statistics calculated using these quartiles to quantify these characteristics precisely. The equations for η_1 and η_2 are provided below:

$$\eta_1 = \frac{Q(0.75)-2Q(0.5)+Q(0.25)}{Q(0.75)-Q(0.25)},$$

and

$$\eta_2 = \frac{Q(0.875) - Q(0.625) - Q(0.375) + Q(0.125)}{Q(0.75) - Q(0.25)}.$$

Table 1 presents quantile values (Q_1, Q_2, Q_3), η_1 and η_2 of the HTPXLD for various parameter values and u values. The table reveals several trends: The data show that increasing ϑ leads to higher values for Q_1, Q_2, and Q_3, while η_1 and η_2 decrease. Values are generally higher at $\beta = 0.5$ compared to $\beta = 0.8$, and there is a consistent trend where Q_1, Q_2, and Q_3 increase with δ, while η_1 and η_2 decrease.

Table 1: Results of Q_1, Q_2, Q_3, η_1, and η_2 linked to the HTPXLD distribution

β	δ	$\vartheta = 1.8$					$\vartheta = 2.5$				
		Q_1	Q_2	Q_3	η_1	η_2	Q_1	Q_2	Q_3	η_1	η_2
0.5	1.3	0.4741	0.8249	1.3384	0.1881	1.2850	0.5843	0.8706	1.2335	0.1179	1.2458
	1.5	0.5738	0.9795	1.5398	0.1600	1.2514	0.6703	0.9851	1.3645	0.0930	1.2252
	1.7	0.6389	1.0766	1.6598	0.1425	1.2353	0.7242	1.0546	1.4402	0.0772	1.2163
	1.9	0.6853	1.1441	1.7405	0.1305	1.2261	0.7618	1.1018	1.4904	0.0668	1.2115
	2.1	0.7204	1.1940	1.7989	0.1217	1.2203	0.7897	1.1362	1.5262	0.0590	1.2088
	2.3	0.7478	1.2326	1.8434	0.1150	1.2163	0.8112	1.1625	1.5532	0.0531	1.2071
	2.5	0.7699	1.2633	1.8783	0.1097	1.2136	0.8284	1.1833	1.5744	0.0485	1.2062
	2.7	0.7881	1.2884	1.9065	0.1054	1.2115	0.8425	1.2001	1.5914	0.0448	1.2055
	3	0.8102	1.3184	1.9400	0.1003	1.2093	0.8593	1.2202	1.6115	0.0404	1.2048
	3.5	0.8373	1.3551	1.9805	0.0942	1.2070	0.8800	1.2445	1.6356	0.0351	1.2044
	3.7	0.8459	1.3665	1.9930	0.0923	1.2063	0.8865	1.2521	1.6430	0.0334	1.2043
	4	0.8570	1.3813	2.0091	0.0898	1.2055	0.8948	1.2618	1.6526	0.0313	1.2042
	4.5	0.8718	1.4009	2.0304	0.0866	1.2045	0.9059	1.2747	1.6652	0.0285	1.2042
	4.7	0.8768	1.4075	2.0375	0.0855	1.2042	0.9097	1.2790	1.6694	0.0277	1.2043
	5	0.8834	1.4163	2.0469	0.0841	1.2038	0.9147	1.2847	1.6749	0.0265	1.2043
0.8	1.3	0.3261	0.5742	0.9497	0.2043	1.3033	0.4463	0.6707	0.9635	0.1323	1.2565
	1.5	0.3958	0.6857	1.1004	0.1772	1.2647	0.5131	0.7621	1.0713	0.1079	1.2316
	1.7	0.4417	0.7565	1.1909	0.1597	1.2454	0.5553	0.8180	1.1341	0.0922	1.2199
	1.9	0.4746	0.8060	1.2521	0.1476	1.2341	0.5847	0.8561	1.1757	0.0815	1.2134
	2.1	0.4995	0.8428	1.2965	0.1385	1.2268	0.6066	0.8841	1.2056	0.0734	1.2095
	2.3	0.5190	0.8712	1.3303	0.1317	1.2217	0.6236	0.9055	1.2281	0.0673	1.2070
	2.5	0.5348	0.8940	1.3569	0.1262	1.2180	0.6372	0.9225	1.2458	0.0625	1.2053
	2.7	0.5478	0.9125	1.3784	0.1218	1.2153	0.6484	0.9362	1.2599	0.0586	1.2041
	3	0.5636	0.9348	1.4040	0.1165	1.2123	0.6617	0.9526	1.2767	0.0539	1.2028
	3.5	0.5831	0.9621	1.4349	0.1100	1.2090	0.6781	0.9726	1.2969	0.0483	1.2016
	3.7	0.5892	0.9706	1.4445	0.1081	1.2080	0.6833	0.9788	1.3032	0.0466	1.2014
	4	0.5972	0.9817	1.4568	0.1054	1.2069	0.6899	0.9868	1.3111	0.0443	1.2009
	4.5	0.6079	0.9963	1.4731	0.1021	1.2054	0.6988	0.9974	1.3217	0.0414	1.2006
	4.7	0.6115	1.0012	1.4786	0.1010	1.2050	0.7017	1.0009	1.3252	0.0403	1.2005
	5	0.6162	1.0078	1.4858	0.0995	1.2045	0.7057	1.0056	1.3299	0.0390	1.2003

3.3 Moments

Moments of distribution offer valuable insights into its shape. They reveal measures like central tendency (average), dispersion (spread), skewness (asymmetry), and kurtosis (peakedness). Therefore, deriving the moments is crucial for understanding any new distribution. The k-th moment about the origin of the HTPXLD is obtained by using PDF (9) as follows:

$$\mu_k' = \sum_{j_1=0}^{\infty} \tau_{j_1,j_2} \vartheta \int_0^{\infty} \left(2+\beta+y^{\vartheta}\right) y^{k+\vartheta(j_2+1)-1} e^{-\beta(j_1+1)y^{\vartheta}} dy$$
$$= \sum_{j_1=0}^{\infty} \tau_{j_1,j_2} \vartheta \left[\int_0^{\infty} (2+\beta) y^{k+\vartheta(j_2+1)-1} e^{-\beta(j_1+1)y^{\vartheta}} dy + \int_0^{\infty} y^{k+\vartheta(j_2+2)-1} e^{-\beta(j_1+1)y^{\vartheta}} dy \right]. \tag{12}$$

Using the transformation $z = \beta(j+1)y^{\vartheta}$ in (12), we have

$$\mu_k' = \sum_{j_1=0}^{\infty} \tau_{j_1,j_2} \left[\frac{(2+\beta)}{\beta(j_1+1)^{j_2+1+(k/\vartheta)}} \int_0^{\infty} z^{j_2+(k/\vartheta)} e^{-z} dz + \frac{1}{\beta(j_1+1)^{j_2+2+(k/\vartheta)}} \int_0^{\infty} z^{j_2+(k/\vartheta)+1} e^{-z} dz \right]$$
$$= \sum_{j_1=0}^{\infty} \frac{\tau_{j_1,j_2} \Gamma\left(j_2+1+(k/\vartheta)\right)}{\beta(j_1+1)^{j_2+1+(k/\vartheta)}} \left[(2+\beta) + \frac{j_2+1+(k/\vartheta)}{\beta(j_1+1)} \right], \tag{13}$$

where $\Gamma(.)$ stands for gamma function (GF). For $n = 1$ in (13), the mean of the HTPXLD is produced. Moreover, the k-th central moment of Y may be calculated in the way that follows by utilizing moments around the origin.

$$\mu_k = E(Y-\mu_1')^k = \sum_{u=0}^{k} (-1)^u \binom{k}{u} \mu_1'^u \mu_{k-u}'.$$

Then, using the formulas, $\kappa_1 = \mu_3/(\mu_2)^{1.5}$ and $\kappa_2 = \mu_4/(\mu_2)^2$, one may find the coefficients of skewness and kurtosis, respectively. They play crucial roles in establishing the asymmetry and flatness of the provided distribution. Also, another important measure is the coefficient of variation (CV), defined by CV $= \frac{\sigma}{\mu_1'}$, where μ_1' is the first moment and σ is the standard deviation.

Likewise, the k-th incomplete moment of the HTPXLD, based on PDF (9), is determined as follows:

$$\lambda_k(x) = \sum_{j_1=0}^{\infty} \tau_{j_1,j_2} \vartheta \int_0^{x} \left(2+\beta+y^{\vartheta}\right) y^{k+\vartheta(j_2+1)-1} e^{-\beta(j_1+1)y^{\vartheta}} dy$$
$$= \sum_{j_1=0}^{x} \tau_{j_1,j_2} \vartheta \left[\int_0^{x} (2+\beta) y^{k+\vartheta(j_2+1)-1} e^{-\beta(j_1+1)y^{\vartheta}} dy + \int_0^{x} y^{k+\vartheta(j_2+2)-1} e^{-\beta(j_1+1)y^{\vartheta}} dy \right]. \tag{14}$$

Using the transformation $z = \beta(j+1)y^{\vartheta}$ in (14), we have

$$\lambda_k(x) = \sum_{j_1=0}^{\infty} \tau_{j_1,j_2} \left[\frac{(2+\beta)}{\beta(j_1+1)^{j_2+1+(k/\vartheta)}} \int_0^{\beta(j+1)x^{\vartheta}} z^{j_2+(k/\vartheta)} e^{-z} dz + \frac{1}{\beta(j_1+1)^{j_2+2+(k/\vartheta)}} \int_0^{\beta(j+1)x^{\vartheta}} z^{j_2+(k/\vartheta)+1} e^{-z} dz \right]$$
$$= \sum_{j_1=0}^{\infty} \tau_{j_1,j_2} \left\{ \frac{(2+\beta)\gamma\left(j_2+(k/\vartheta)+1, \beta(j+1)x^{\vartheta}\right)}{\left[\beta(j_1+1)\right]^{j_2+(k/\vartheta)+1}} + \frac{\gamma\left(j_2+(k/\vartheta)+2, \beta(j+1)x^{\vartheta}\right)}{\left[\beta(j_1+1)\right]^{j_2+(k/\vartheta)+2}} \right\}, \tag{15}$$

where $\gamma(.,x)$ is the lower incomplete GF. One can find applications of incomplete moments by [44].

Tables 2 and 3 present numerical outcomes for the first four moments, variance (σ^2), σ, κ_1, κ_2 and CV for the HTPXLD for some selected parameter values. Based on the positive values of $\kappa_1 > 0$, the HTPXLD exhibits right-skewed. The distribution is characterized as leptokurtic for $\kappa_1 > 3$ and platykurtic for $\kappa_1 < 3$.

Table 2: Numerical outcomes for the first four moments, σ^2, σ, κ_1, κ_2 and CV for the HTPXLD when $\vartheta = 1.8$

β	δ	μ_1'	μ_2'	μ_3'	μ_4'	σ^2	σ	κ_1	κ_2	CV
0.5	1.3	0.9933	1.4831	2.9200	7.0059	0.4965	0.7046	1.3160	5.1272	0.7094
	1.5	1.1373	1.8574	3.8658	9.5912	0.5639	0.7509	1.1118	4.4033	0.6603
	1.7	1.2252	2.1029	4.5182	11.4361	0.6017	0.7757	1.0014	4.0682	0.6331
	1.9	1.2855	2.2785	4.9993	12.8259	0.6260	0.7912	0.9309	3.8745	0.6155
	2.1	1.3297	2.4110	5.3701	13.9130	0.6430	0.8018	0.8815	3.7483	0.6030
	2.3	1.3636	2.5148	5.6651	14.7878	0.6555	0.8096	0.8447	3.6596	0.5938
	2.5	1.3905	2.5986	5.9058	15.5074	0.6652	0.8156	0.8163	3.5940	0.5866
	2.7	1.4123	2.6676	6.1061	16.1102	0.6728	0.8203	0.7935	3.5434	0.5808
	3	1.4385	2.7510	6.3505	16.8509	0.6818	0.8257	0.7669	3.4862	0.5740
	3.5	1.4703	2.8542	6.6559	17.7838	0.6923	0.8320	0.7351	3.4210	0.5659
	3.7	1.4803	2.8867	6.7529	18.0819	0.6955	0.8340	0.7253	3.4016	0.5634
	4	1.4931	2.9288	6.8788	18.4699	0.6996	0.8364	0.7128	3.3774	0.5602
	4.5	1.5101	2.9852	7.0488	18.9958	0.7049	0.8396	0.6964	3.3462	0.5560
	4.7	1.5157	3.0041	7.1060	19.1733	0.7066	0.8406	0.6909	3.3361	0.5546
	5	1.5233	3.0294	7.1827	19.4119	0.7089	0.8420	0.6837	3.3228	0.5527
0.8	1.3	0.7066	0.7715	1.1319	2.0463	0.2722	0.5218	1.4226	5.5391	0.7384
	1.5	0.8125	0.9722	1.5075	2.8149	0.3120	0.5586	1.2082	4.7125	0.6875
	1.7	0.8775	1.1047	1.7682	3.3664	0.3347	0.5785	1.0927	4.3285	0.6593
	1.9	0.9221	1.1998	1.9612	3.7833	0.3494	0.5911	1.0189	4.1058	0.6410
	2.1	0.9550	1.2717	2.1103	4.1101	0.3598	0.5998	0.9672	3.9602	0.6281
	2.3	0.9802	1.3282	2.2292	4.3736	0.3675	0.6062	0.9288	3.8577	0.6185
	2.5	1.0002	1.3739	2.3264	4.5907	0.3734	0.6111	0.8991	3.7816	0.6110
	2.7	1.0165	1.4115	2.4073	4.7727	0.3782	0.6150	0.8754	3.7229	0.6050
	3	1.0360	1.4571	2.5061	4.9966	0.3837	0.6194	0.8476	3.6563	0.5979
	3.5	1.0598	1.5135	2.6299	5.2789	0.3903	0.6247	0.8144	3.5803	0.5894
	3.7	1.0673	1.5313	2.6692	5.3692	0.3923	0.6263	0.8043	3.5576	0.5868
	4	1.0768	1.5543	2.7203	5.4868	0.3948	0.6283	0.7913	3.5292	0.5835
	4.5	1.0895	1.5852	2.7893	5.6463	0.3982	0.6310	0.7741	3.4926	0.5791
	4.7	1.0938	1.5956	2.8125	5.7002	0.3993	0.6319	0.7685	3.4807	0.5777
	5	1.0994	1.6095	2.8437	5.7726	0.4007	0.6330	0.7610	3.4651	0.5758

Table 3: Numerical outcomes for the first four moments, σ^2, σ, κ_1, κ_2 and CV for the HTPXLD when $\vartheta = 2.5$

β	δ	μ_1'	μ_2'	μ_3'	μ_4'	σ^2	σ	κ_1	κ_2	CV
0.5	1.3	0.9477	1.1376	1.6265	2.6607	0.2395	0.4894	0.8062	3.5801	0.5164
	1.5	1.0500	1.3617	2.0591	3.5040	0.2593	0.5092	0.6428	3.2292	0.4850
	1.7	1.1109	1.5034	2.3456	4.0827	0.2693	0.5189	0.5521	3.0729	0.4671

(Continued)

Table 3 (continued)

β	δ	μ_1'	μ_2'	μ_3'	μ_4'	σ^2	σ	κ_1	κ_2	CV
	1.9	1.1521	1.6025	2.5517	4.5081	0.2753	0.5247	0.4932	2.9860	0.4554
	2.1	1.1819	1.6762	2.7078	4.8353	0.2792	0.5284	0.4515	2.9315	0.4471
	2.3	1.2047	1.7333	2.8304	5.0952	0.2820	0.5310	0.4203	2.8945	0.4408
	2.5	1.2226	1.7789	2.9296	5.3070	0.2841	0.5330	0.3959	2.8680	0.4359
	2.7	1.2372	1.8163	3.0114	5.4830	0.2857	0.5345	0.3764	2.8481	0.4320
	3	1.2545	1.8612	3.1105	5.6977	0.2874	0.5361	0.3534	2.8264	0.4274
	3.5	1.2755	1.9163	3.2333	5.9656	0.2894	0.5380	0.3258	2.8026	0.4218
	3.7	1.2820	1.9336	3.2721	6.0507	0.2900	0.5385	0.3173	2.7958	0.4201
	4	1.2904	1.9558	3.3222	6.1610	0.2908	0.5392	0.3065	2.7875	0.4179
	4.5	1.3015	1.9856	3.3896	6.3098	0.2917	0.5401	0.2921	2.7771	0.4150
	4.7	1.3052	1.9956	3.4122	6.3599	0.2920	0.5404	0.2873	2.7738	0.4140
	5	1.3101	2.0088	3.4424	6.4270	0.2924	0.5407	0.2810	2.7696	0.4127
0.8	1.3	0.7393	0.7031	0.8063	1.0677	0.1565	0.3956	0.8914	3.7799	0.5351
	1.5	0.8218	0.8462	1.0273	1.4146	0.1709	0.4134	0.7223	3.3723	0.5030
	1.7	0.8711	0.9372	1.1745	1.6542	0.1784	0.4223	0.6285	3.1875	0.4848
	1.9	0.9045	1.0010	1.2807	1.8310	0.1829	0.4277	0.5676	3.0832	0.4728
	2.1	0.9288	1.0486	1.3615	1.9674	0.1860	0.4312	0.5246	3.0169	0.4643
	2.3	0.9473	1.0856	1.4251	2.0759	0.1881	0.4338	0.4923	2.9712	0.4579
	2.5	0.9620	1.1152	1.4765	2.1645	0.1898	0.4356	0.4672	2.9381	0.4529
	2.7	0.9738	1.1394	1.5190	2.2382	0.1910	0.4371	0.4471	2.9130	0.4488
	3	0.9880	1.1686	1.5706	2.3281	0.1925	0.4387	0.4234	2.8852	0.4440
	3.5	1.0051	1.2044	1.6345	2.4406	0.1941	0.4406	0.3949	2.8544	0.4383
	3.7	1.0105	1.2156	1.6547	2.4763	0.1946	0.4411	0.3862	2.8455	0.4365
	4	1.0173	1.2301	1.6809	2.5227	0.1952	0.4418	0.3750	2.8344	0.4343
	4.5	1.0264	1.2495	1.7160	2.5853	0.1960	0.4427	0.3602	2.8205	0.4313
	4.7	1.0294	1.2560	1.7278	2.6064	0.1962	0.4430	0.3552	2.8160	0.4303
	5	1.0335	1.2646	1.7436	2.6346	0.1966	0.4433	0.3487	2.8102	0.4290

Tables 2 and 3 reveal several trends: As β and δ increase, it κ_1 shows a decrease in kurtosis, with values in Table 3 being lower than those in Table 2, indicating reduced kurtosis at $\vartheta = 2.5$ compared to $\vartheta = 1.8$. The values of σ^2, σ, and CV follow similar trends across the tables, increasing with higher β and δ in both cases.

3.4 Stochastic Ordering

A concept in probability distributions that has been studied in great detail is stochastic ordering, which is crucial for analyzing comparative behavior among random variables in reliability theory and other fields. Stochastic ordering is a powerful tool used in probability and statistics to compare the behavior of random variables. It allows us to understand which random variable is "less risky" or has a "lower probability of taking on extreme values" compared to another. A random variable Y_1 is regarded as less than a random variable Y_2 in the following ways:

- SO (represented by $Y_1 \leq_{st} Y_2$) if $F_{Y_1}(y) \geq F_{Y_2}(y)\ \forall\ y$.
- hazard rate order (represented by $Y_1 \leq_{hr} Y_2$) if $h_{Y_1}(y) \geq h_{Y_2}(y)\ \forall\ y$.

- likelihood ratio order (represented by $Y_1 \leq_{lr} Y_2$) if $\frac{f_{Y_1}(y)}{f_{Y_2}(y)}$ decreases in y.

According to Shaked et al. [45], the following impacts are widely recognized:

$Y_1 \leq_{lr} Y_2 \Rightarrow Y_1 \leq_{hr} Y_2 \Rightarrow Y_1 \leq_{st} Y_2$.

Let $Y_1 \sim$ HTPXLD (ω_1), $\omega_1 \equiv (\delta_1, \beta, \vartheta_1)$ and $Y_2 \sim$ HTPXLD (ω_2), $\omega_2 \equiv (\delta_2, \beta, \vartheta_2)$, then the likelihood ratio ordering is as follows:

$$\frac{f_1(y;\omega_1)}{f_2(y;\omega_2)} = \frac{\delta_1(\delta_1-1)\vartheta_1(2+\beta+y^{\vartheta_1})y^{\vartheta_1-1}e^{-\beta y^{\vartheta_1}}\left[\delta_2-\left(1+\beta^{\bullet}y^{\vartheta_2}\right)e^{-\beta y^{\vartheta_2}}\right]^2}{\delta_2(\delta_2-1)\vartheta_2(2+\beta+y^{\vartheta_2})y^{\vartheta_2-1}e^{-\beta y^{\vartheta_2}}\left[\delta_1-(1+\beta^{\bullet}y^{\vartheta_1})e^{-\beta y^{\vartheta_1}}\right]^2},$$

then

$$\frac{d}{dy}\log\left[\frac{f_1(y;\omega_1)}{f_2(y;\omega_2)}\right] = \frac{\vartheta_1\, y^{\vartheta_1-1}}{(2+\beta+y^{\vartheta_1})} - \frac{\vartheta_2\, y^{\vartheta_2-1}}{(2+\beta+y^{\vartheta_2})} - \frac{2\vartheta_2 y^{\vartheta_2-1}e^{-\beta y^{\vartheta_2}}\left[\beta^{\bullet}-\beta\left(1+\beta^{\bullet}y^{\vartheta_2}\right)\right]}{\left[\delta_2-(1+\beta^{\bullet}y^{\vartheta_2})e^{-\beta y^{\vartheta_2}}\right]} - \frac{\vartheta_2-1}{y}$$
$$+\frac{\vartheta_1-1}{y} - \beta\vartheta_1 y^{\vartheta_1-1} + \beta\vartheta_2 y^{\vartheta_2-1} + \frac{2\vartheta_1 y^{\vartheta_1-1}e^{-\beta y^{\vartheta_1}}\left[\beta^{\bullet}-\beta\left(1+\beta^{\bullet}y^{\vartheta_1}\right)\right]}{\left[\delta_2-(1+\beta^{\bullet}y^{\vartheta_1})e^{-\beta y^{\vartheta_1}}\right]}.$$

For $\vartheta_2 < \vartheta_1$, $\delta_2 < \delta_1$, we get $\frac{d}{dy}\log\left[\frac{f_1(y;\omega_1)}{f_2(y;\omega_2)}\right] < 0$, for all $y \geq 0$, hence $\frac{d}{dy}\log\left[\frac{f_1(y;\omega_1)}{f_2(y;\omega_2)}\right] < 0$, is decreasing in y and hence $Y_1 \leq_{lr} Y_2$.

3.5 Extropy Measures

The extropy (Ext), which is the double complement of the entropy [46], was developed as an alternative uncertainty measure by Lad et al. [47]. The Ext can be statistically utilized to evaluate the accuracy of predicted distributions through the total log scoring method. For a non-negative random variable$Y$, Ext is defined as follows:

$$\Xi = \frac{-1}{2}\int_0^{\infty} f^2(y)dy. \tag{16}$$

Thus, using PDF (6) in (16), the extropy of the HTPXLD may be represented as follows:

$$\Xi = \frac{-1}{2\delta^2}\int_0^{\infty}(\beta^{\bullet}\vartheta(\delta-1)\beta)^2(2+\beta+y^{\vartheta})^2 y^{2(\vartheta-1)}e^{-2\beta y^{\vartheta}}\left[1-\frac{\left(1+\beta^{\bullet}y^{\vartheta}\right)e^{-\beta y^{\vartheta}}}{\delta}\right]^{-4}dy. \tag{17}$$

Using the expansion (7) in (17) gives

$$\Xi = \frac{-1}{2}\sum_{j_1=0}^{\infty}\frac{(-1)^{j_1}(\beta^{\bullet}(\delta-1)\vartheta\beta)^2}{\delta^{2+j_1}}\binom{3+j_1}{j_1}\int_0^{\infty}(2+\beta+y^{\vartheta})^2 y^{2(\vartheta-1)}e^{-2\beta y^{\vartheta}}\left(1+\beta^{\bullet}y^{\vartheta}\right)^{j_1}e^{-\beta j_1 y^{\vartheta}}dy. \tag{18}$$

Using binomial expansion in (18), we have

$$\Xi = \frac{-1}{2}\sum_{j_1=0}^{\infty}\sum_{j_2=0}^{j_1}\binom{3+j_1}{j_1}\binom{j_2}{j_1}\frac{(-1)^{j_1}(\beta^{\bullet})^{2+j}(\vartheta(\delta-1)\beta)^2}{\delta^{2+j_1}}\int_0^{\infty}(2+\beta+y^{\vartheta})^2 y^{2(\vartheta-1)+\vartheta j_2}e^{-(2\beta+\beta j_1)y^{\vartheta}}dy,$$

Then after some simplified form, the previous equation will be

$$\Xi = \frac{-1}{2}\sum_{j_1=0}^{\infty} p_{j_1.j_2}\vartheta\left[\int_0^{\infty}(2+\beta)^2 y^{2(\vartheta-1)+\vartheta j_2} e^{-(2\beta+\beta j_1)y^{\vartheta}}dy + (2+\beta)\int_0^{\infty} y^{2(\vartheta-1)+\vartheta j_2+\vartheta} e^{-(2\beta+\beta j_1)y^{\vartheta}}dy + \int_0^{\infty} y^{2(2\vartheta-1)+\vartheta j_2} e^{-(2\beta+\beta j_1)y^{\vartheta}}dy\right]. \quad (19)$$

Using the transformation $z = \beta(j+1)y^{\vartheta}$ in (19), the extropy measure of HTPXLD thus has the following structure after some simplification:

$$\Xi = \frac{-1}{2}\sum_{j_1=0}^{\infty} p_{j_1.j_2}\left[\frac{(2+\beta)^2\Gamma(2+j_2-(1/\vartheta))}{(2\beta+\beta j_1)^{(2+j_2-(1/\vartheta))}} + \frac{(2+\beta)\Gamma(3+j_2-(1/\vartheta))}{(2\beta+\beta j_1)^{(3+j_2-(1/\vartheta))}} + \frac{\Gamma(4+j_2-(1/\vartheta))}{(2\beta+\beta j_1)^{(4+j_2-(1/\vartheta))}}\right],$$

where $p_{j_1.j_2} = \sum_{j_2=0}^{j_1}\binom{3+j_1}{j_1}\binom{j_2}{j_1}\frac{(-1)^{j_1}(\beta^{\bullet})^{2+j}\vartheta((\delta-1)\beta)^2}{\delta^{2+j_1}}$.

Weighted extropy (WExt), introduced by [48], offers an alternative perspective to traditional entropy. Unlike entropy, it assigns greater weight to larger values within a probability distribution. It can be expressed, mathematically, by

$$\Xi_w = \frac{-1}{2}\int_0^{\infty} y f^2(y)dy. \quad (20)$$

Then by inserting PDF (6) in (20), then the WExt is

$$\Xi_w = \frac{-1}{2\delta^2}\int_0^{\infty}(\beta^{\bullet}\vartheta(\delta-1)\beta)^2(2+\beta+y^{\vartheta})^2 y^{2\vartheta-1}e^{-2\beta y^{\vartheta}}\left[1-\frac{(1+\beta^{\bullet}y^{\vartheta})e^{-\beta y^{\vartheta}}}{\delta}\right]^{-4}dy.$$

Using the similar procedure discussed above, then Ξ_w is as follows:

$$\Xi_w = \frac{-1}{2}\sum_{j_1=0}^{\infty} p_{j_1.j_2}\left[\frac{(2+\beta)^2\Gamma(2+j_2)}{(2\beta+\beta j_1)^{(2+j_2)}} + \frac{(2+\beta)\Gamma(3+j_2)}{(2\beta+\beta j_1)^{(3+j_2)}} + \frac{\Gamma(4+j_2)}{(2\beta+\beta j_1)^{(4+j_2)}}\right].$$

The residual extropy (RExt) at the time t of residual lifespan Z_t is given by

$$\Xi_R = \frac{-1}{2\bar{G}^2(t)}\int_t^{\infty} f^2(z)dz. \quad (21)$$

Then, by inserting PDF (6) in (21) and using the similar procedure discussed above, the RExt will be

$$\Xi_R = \frac{-1}{2\bar{G}^2(t)}\sum_{j_1=0}^{\infty} p_{j_1.j_2}\left[\frac{(2+\beta)^2\Gamma\left(2+j_2-(1/\vartheta),(2\beta+\beta j_1)t^{\vartheta}\right)}{(2\beta+\beta j_1)^{(2+j_2-(1/\vartheta))}} + \frac{(2+\beta)\Gamma\left(3+j_2-(1/\vartheta),(2\beta+\beta j_1)t^{\vartheta}\right)}{(2\beta+\beta j_1)^{(3+j_2-(1/\vartheta))}} + \frac{\Gamma\left(4+j_2-(1/\vartheta),(2\beta+\beta j_1)t^{\vartheta}\right)}{(2\beta+\beta j_1)^{(4+j_2-(1/\vartheta))}}\right],$$

where $\Gamma(., x)$ is the upper incomplete GF. According to Table 4, for both values of ϑ, there is a discernible trend in the Ext and RExt measures towards becoming less negative with rising β. Both Ext and RExt exhibit a decline in negativity as β rises. On the other hand, WExt's negativity steadily drops as β rises. When $\vartheta = 2.5$ is used instead of $\vartheta = 1.8$, the decline in WExt is more gradual and more noticeable at higher β values.

Table 4: The Extropy metrics for the HTPXLD distribution

β	δ	$\vartheta = 1.8$				$\vartheta = 2.5$			
		Ext	WExt	RExt		Ext	WExt	RExt	
				$t = 0.8$	$t = 1.2$			$t = 0.8$	$t = 1.2$
0.5	1.3	−0.2515	−0.1852	−0.3412	−0.3633	−0.3098	−0.2573	−0.4791	−0.5849
	1.5	−0.2204	−0.1963	−0.3024	−0.3366	−0.2871	−0.2727	−0.4291	−0.5495
	1.7	−0.2060	−0.2039	−0.2814	−0.3201	−0.2769	−0.2832	−0.4030	−0.5273
	1.9	−0.1977	−0.2095	−0.2683	−0.3090	−0.2712	−0.2909	−0.3870	−0.5121
	2.1	−0.1923	−0.2137	−0.2593	−0.3010	−0.2677	−0.2969	−0.3762	−0.5011
	2.3	−0.1885	−0.2171	−0.2527	−0.2949	−0.2652	−0.3016	−0.3685	−0.4927
	2.5	−0.1858	−0.2199	−0.2477	−0.2902	−0.2635	−0.3054	−0.3627	−0.4862
	2.7	−0.1836	−0.2222	−0.2439	−0.2864	−0.2622	−0.3086	−0.3582	−0.4809
	3.0	−0.1812	−0.2250	−0.2394	−0.2819	−0.2607	−0.3125	−0.3530	−0.4746
	3.5	−0.1784	−0.2285	−0.2341	−0.2766	−0.2591	−0.3173	−0.3471	−0.4671
	3.7	−0.1776	−0.2296	−0.2326	−0.2749	−0.2587	−0.3188	−0.3453	−0.4648
	4.0	−0.1765	−0.2310	−0.2306	−0.2728	−0.2581	−0.3208	−0.3431	−0.4618
	4.5	−0.1752	−0.2329	−0.2280	−0.2701	−0.2574	−0.3235	−0.3402	−0.4579
	4.7	−0.1748	−0.2336	−0.2271	−0.2691	−0.2572	−0.3244	−0.3393	−0.4566
	5.0	−0.1742	−0.2344	−0.2260	−0.2679	−0.2569	−0.3256	−0.3380	−0.4549
0.8	1.3	−0.3537	−0.1793	−0.4811	−0.5077	−0.3917	−0.2491	−0.6600	−0.8068
	1.5	−0.3068	−0.1892	−0.4420	−0.4874	−0.3598	−0.2627	−0.6063	−0.7812
	1.7	−0.2849	−0.1960	−0.4184	−0.4736	−0.3451	−0.2722	−0.5749	−0.7636
	1.9	−0.2723	−0.2010	−0.4026	−0.4636	−0.3368	−0.2792	−0.5543	−0.7506
	2.1	−0.2640	−0.2049	−0.3913	−0.4560	−0.3315	−0.2845	−0.5398	−0.7407
	2.3	−0.2582	−0.2080	−0.3828	−0.4501	−0.3278	−0.2888	−0.5290	−0.7329
	2.5	−0.2539	−0.2105	−0.3762	−0.4454	−0.3252	−0.2923	−0.5208	−0.7266
	2.7	−0.2506	−0.2126	−0.3709	−0.4414	−0.3232	−0.2953	−0.5142	−0.7214
	3.0	−0.2468	−0.2151	−0.3647	−0.4367	−0.3209	−0.2988	−0.5065	−0.7151
	3.5	−0.2425	−0.2183	−0.3573	−0.4309	−0.3184	−0.3033	−0.4975	−0.7073
	3.7	−0.2413	−0.2194	−0.3550	−0.4291	−0.3177	−0.3047	−0.4947	−0.7049
	4.0	−0.2397	−0.2207	−0.3521	−0.4267	−0.3168	−0.3065	−0.4912	−0.7017
	4.5	−0.2376	−0.2225	−0.3484	−0.4236	−0.3157	−0.3090	−0.4866	−0.6975
	4.7	−0.2369	−0.2231	−0.3471	−0.4225	−0.3153	−0.3098	−0.4851	−0.6961
	5.0	−0.2360	−0.2239	−0.3454	−0.4211	−0.3148	−0.3109	−0.4831	−0.6942

3.6 Stress-Strength Model

The SS model is a powerful tool in reliability engineering used to assess the probability of a component surviving under operational conditions. It considers two random variables: strength (X), which stands for the component's intrinsic ability to withstand stress (Y). Therefore, the core concept of the SS model is captured by the following equation: $R = P(Y < X)$, where R represents the reliability, or the probability of the component functioning successfully. This model has a wide range of applications across various scientific fields. Let the strength $X \sim$ HTPXLD $(\delta_1, \beta_1, \vartheta)$ and stress $Y \sim$ HTPXLD $(\delta_2, \beta_2, \vartheta)$, then the SS parameter for the HTPXLD is given by

$$R = \int_0^{\infty} \frac{\delta_1(\delta_1 - 1)\beta_1^{\bullet}\vartheta\beta_1(2 + \beta_1 + x^{\vartheta})x^{\vartheta-1}e^{-\beta_1 x^{\vartheta}}}{\left[\delta_1 - (1 + \beta_1^{\bullet}x^{\vartheta})\, e^{-\beta_1 x^{\vartheta}}\right]^2} \frac{\delta_2\left[1 - \left(1 + \beta_2^{\bullet}x^{\vartheta}\right) e^{-\beta_2 x^{\vartheta}}\right]}{\delta_2 - \left(1 + \beta_2^{\bullet}x^{\vartheta}\right) e^{-\beta_2 x^{\vartheta}}} dx, \tag{22}$$

where $\beta_1^{\bullet} = \frac{\beta_1}{(1+\beta_1)^2}$, and $\beta_2^{\bullet} = \frac{\beta_2}{(1+\beta_2)^2}$. Using expansion (7) twice for the numerator of Eq. (22) gives

$$\begin{aligned} R = &\sum_{u_1,u_2=0}^{\infty} \mathrm{A}^* \int_0^{\infty} \vartheta(2 + \beta_1 + x^{\vartheta})\left(1 + \beta_1^{\bullet}x^{\vartheta}\right)^{u_1}\left(1 + \beta_2^{\bullet}x^{\vartheta}\right)^{u_2} x^{\vartheta-1}e^{-[\beta_1(u_1+1)+\beta_2 u_2]x^{\vartheta}} \\ &\times\left[1 - \left(1 + \beta_2^{\bullet}x^{\vartheta}\right) e^{-\beta_2 x^{\vartheta}}\right] dx, \end{aligned} \tag{23}$$

where $\mathrm{A}^* = \frac{(-1)^{u_1+u_2}(u_1+1)\beta_1\beta_1^{\bullet}}{(\delta_1)^{u_1+1}(\delta_2)^{u_2}}$. Again, employing the binomial expansion in (23), we get

$$\begin{aligned} R = &\sum_{u_1,u_2=0}^{\infty}\sum_{v_1=0}^{u_1}\sum_{v_2=0}^{u_2}\binom{u_1}{v_1}\binom{u_2}{v_2}\mathrm{A}^*\int_0^{\infty}\vartheta(2 + \beta_1 + x^{\vartheta})(\beta_1^{\bullet})^{v_1}x^{v_1\vartheta}(\beta_2^{\bullet})^{v_2}x^{v_2\vartheta}x^{\vartheta-1}e^{-\beta_1(u_1+u_2+1)x^{\vartheta}}dx \\ &- \sum_{u_1,u_2=0}^{\infty}\sum_{v_1=0}^{u_1}\sum_{v_2=0}^{u_2}\binom{u_1}{v_1}\binom{u_2+1}{v_2}\mathrm{A}^*\int_0^{\infty}\vartheta(2 + \beta_1 + x^{\vartheta})\beta_1^{\bullet})^{v_1}x^{v_1\vartheta}(\beta_2^{\bullet})^{v_2}x^{v_2\vartheta}x^{\vartheta-1}e^{-[\beta_1(u_1+u_2+1)+\beta_2]x^{\vartheta}}\, dx. \end{aligned} \tag{24}$$

After simplifying Eq. (24), we get

$$\begin{aligned} R = &\sum_{u_1,u_2=0}^{\infty}\mathrm{A}^{**}\int_0^{\infty}\vartheta(2 + \beta_1 + x^{\vartheta})(\beta_1^{\bullet})^{v_1}x^{v_1\vartheta}(\beta_2^{\bullet})^{v_2}x^{v_2\vartheta}x^{\vartheta-1}e^{-[\beta_1(u_1+1)+\beta_2(u_2+1)]x^{\vartheta}}dx \\ &- \sum_{u_1,u_2=0}^{\infty}\mathrm{B}^{**}\int_0^{\infty}\vartheta(2 + \beta_1 + x^{\vartheta})(\beta_1^{\bullet})^{v_1}x^{v_1\vartheta}(\beta_2^{\bullet})^{v_2}x^{v_2\vartheta}x^{\vartheta-1}e^{-[\beta_1(u_1+1)+\beta_2(u_2+1)]x^{\vartheta}}\, dx, \end{aligned} \tag{25}$$

where $\mathrm{A}^{**} = \sum_{v_1=0}^{u_1}\sum_{v_2=0}^{u_2}\binom{u_1}{v_1}\binom{u_2}{v_2}\mathrm{A}^*$ and $\mathrm{B}^{**} = \sum_{v_1=0}^{u_1}\sum_{v_2=0}^{u_2}\binom{u_1}{v_1}\binom{u_2+1}{v_2}\mathrm{A}^*$.

Note that the integrals in Eq. (25) can be obtained as follows:

$$\begin{aligned} I_1 &= \sum_{u_1,u_2=0}^{\infty}\mathrm{A}^{**}\int_0^{\infty}\vartheta(2 + \beta_1)(\beta_1^{\bullet})^{v_1}x^{v_1\vartheta+v_2\vartheta+\vartheta-1}(\beta_2^{\bullet})^{v_2}e^{-\beta_1(u_1+u_2+1)x^{\vartheta}}dx \\ &= \sum_{u_1,u_2=0}^{\infty}\frac{\mathrm{A}^{**}(2 + \beta_1)(\beta_1^{\bullet})^{v_1}(\beta_2^{\bullet})^{v_2}\Gamma(v_1 + v_2 + 1)}{[\beta_1(u_1 + u_2 + 1)]^{v_1+v_2+1}}, \\ I_2 &= \sum_{u_1,u_2=0}^{\infty}\mathrm{A}^{**}\int_0^{\infty}\vartheta(\beta_1^{\bullet})^{v_1}x^{v_1\vartheta+v_2\vartheta+2\vartheta-1}(\beta_2^{\bullet})^{v_2}e^{-\beta_1(u_1+u_2+1)x^{\vartheta}}dx \end{aligned}$$

$$= \sum_{u_1,u_2=0}^{\infty} \frac{A^{**}(\beta_1^{\bullet})^{\nu_1}(\beta_2^{\bullet})^{\nu_2}\Gamma(\nu_1+\nu_2+2)}{[\beta_1(u_1+u_2+1)]^{\nu_1+\nu_2+2}},$$

$$I_3 = \sum_{u_1,u_2=0}^{\infty} B^{**}\int_0^{\infty} \vartheta(2+\beta_1)\beta_1^{\bullet})^{\nu_1} x^{\nu_1\vartheta+\nu_2\vartheta+\vartheta-1}(\beta_2^{\bullet})^{\nu_2} x^{\nu_2\vartheta} e^{-[\beta_1(u_1+u_2+1)+\beta_2]x^{\vartheta}}$$

$$= \sum_{u_1,u_2=0}^{\infty} \frac{B^{**}(2+\beta_1)(\beta_1^{\bullet})^{\nu_1}(\beta_2^{\bullet})^{\nu_2}\Gamma(\nu_1+\nu_2+1)}{[\beta_1(u_1+u_2+1)+\beta_2]^{\nu_1+\nu_2+1}},$$

and

$$I_4 = \sum_{u_1,u_2=0}^{\infty} B^{**}\int_0^{\infty} \vartheta(\beta_1^{\bullet})^{\nu_1} x^{\nu_1\vartheta+\nu_2\vartheta+2\vartheta-1}(\beta_2^{\bullet})^{\nu_2} e^{-[\beta_1(u_1+u_2+1)+\beta_2]x^{\vartheta}}\,dx,$$

$$= \sum_{u_1,u_2=0}^{\infty} \frac{B^{**}(\beta_1^{\bullet})^{\nu_1}(\beta_2^{\bullet})^{\nu_2}\Gamma(\nu_1+\nu_2+2)}{[\beta_1(u_1+u_2+1)+\beta_2]^{\nu_1+\nu_2+2}}.$$

Then, by inserting I_1, I_2, I_3 and I_4, in the Eq. (25), the SS parameter of HTPXLD is as follows:

$$R = \sum_{u_1,u_2=0}^{\infty}\left[\frac{(2+\beta_1)A^{**}(\beta_1^{\bullet})^{\nu_1}(\beta_2^{\bullet})^{\nu_2}\Gamma(\nu_1+\nu_2+1)}{[\beta_1(u_1+1)+\beta_2 u_2]^{\nu_1+\nu_2+1}} + \frac{A^{**}(\beta_1^{\bullet})^{\nu_1}(\beta_2^{\bullet})^{\nu_2}\Gamma(\nu_1+\nu_2+2)}{[\beta_1(u_1+1)+\beta_2 u_2]^{\nu_1+\nu_2+2}}\right]$$
$$- \sum_{u_1,u_2=0}^{\infty}\left[\frac{(2+\beta_1)B^{**}(\beta_1^{\bullet})^{\nu_1}(\beta_2^{\bullet})^{\nu_2}\Gamma(\nu_1+\nu_2+1)}{[\beta_1(u_1+1)+\beta_2(u_2+1)]^{\nu_1+\nu_2+1}} + \frac{B^{**}(\beta_1^{\bullet})^{\nu_1}(\beta_2^{\bullet})^{\nu_2}\Gamma(\nu_1+\nu_2+2)}{[\beta_1(u_1+1)+\beta_2(u_2+1)]^{\nu_1+\nu_2+2}}\right].$$

4 Actuarial Measures

This section introduces several well-known risk measures for the developed model. These measures include Value-at-Risk (VaR), Tail Value-at-Risk (TVaR), Tail Variance (TV), and Tail Variance Premium (TVP).

4.1 Value-at-Risk

As outlined in reference [49], the q-th quantile of a random variable's CDF corresponds to its VaR. The VaR for the HTPXLD is given by

$$\mathrm{VaR} = \left[-\frac{(\beta+1)^2}{\beta} - \frac{1}{\beta}\; W_{-1}\left\{\left(\tfrac{q\delta-\delta}{q-\delta}\right)(\beta+1)^2 e^{-(\beta+1)^2}\right\}\;\right]^{1/\vartheta}. \tag{26}$$

4.2 Tail Value-at-Risk

TVaR is a crucial risk measure that evaluates the expected loss beyond a specified probability level, once an event has occurred. For the HTPXLD, the TVaR is defined as

$$\mathrm{TVaR} = \frac{1}{1-q}\int_{\mathrm{VaR}_q}^{\infty} y f(y;\omega)\,dy.$$

4.3 Tail Variance and Tail Variance Premium

Landsman [50] first introduced the TV risk measure, which is defined by the variance of the loss distribution above a certain critical threshold. The TV for the HTPXLD can be expressed as

$$\mathrm{TV} = E(Y^2 \mid Y > y_q) - (\mathrm{TVaR})^2.$$

4.4 Tail Variance Premium

The TVP combines statistics related to both the central tendency and dispersion of the data, making it a significant risk measure. The TVP for the HTPXLD is given by

$$\text{TVP} = \text{TVaR} + \kappa \text{TV}, \quad \kappa > 0.$$

Table 5 demonstrates several key trends: Increasing ϑ values lead to higher VaR and TVaR values, indicating an overall increase in risk measures. For example, higher ϑ values correspond to higher risk estimates. For a given δ, higher ϑ results in greater TVP values across all κ levels. This indicates a more pronounced sensitivity to risk with increasing ϑ. Within the same ϑ and δ settings, TVP values rise with κ, reflecting a higher quantile level and, consequently, increased risk assessment.

Table 5: Actuarial measures for $\beta = 0.5$

ϑ	δ	q	VaR	TVaR	TV	TVP		
						$\kappa = 0.50$	$\kappa = 0.75$	$\kappa = 0.90$
1.2	1.3	0.900	2.7485	4.1237	1.8060	5.0267	5.4782	5.7491
		0.910	2.8932	4.2686	1.7965	5.1669	5.6160	5.8855
		0.920	3.0559	4.4306	1.7847	5.3229	5.7691	6.0368
		0.930	3.2414	4.6140	1.7699	5.4990	5.9415	6.2070
		0.940	3.4563	4.8254	1.7516	5.7012	6.1391	6.4018
		0.950	3.7112	5.0745	1.7285	5.9388	6.3709	6.6302
		0.960	4.0234	5.3778	1.6987	6.2271	6.6518	6.9066
		0.970	4.4248	5.7654	1.6593	6.5951	7.0099	7.2589
		0.980	4.9858	6.3047	1.6035	7.1065	7.5073	7.7479
		0.990	5.9258	7.2052	1.5131	7.9618	8.3401	8.5670
		0.995	6.8374	8.0788	1.4316	8.7946	9.1525	9.3672
		0.999	8.8470	10.0138	1.2841	10.6559	10.9769	11.1696
	2.1	0.900	3.8078	5.2073	1.7661	6.0903	6.5319	6.7968
		0.910	3.9634	5.3543	1.7459	6.2273	6.6637	6.9256
		0.920	4.1363	5.5176	1.7238	6.3795	6.8104	7.0690
		0.930	4.3307	5.7012	1.7002	6.5513	6.9764	7.2314
		0.940	4.5532	5.9116	1.6729	6.7481	7.1663	7.4172
		0.950	4.8137	6.1580	1.6422	6.9791	7.3896	7.6359
		0.960	5.1284	6.4561	1.6063	7.2592	7.6608	7.9018
		0.970	5.5280	6.8350	1.5629	7.6165	8.0072	8.2417
		0.980	6.0795	7.3594	1.5067	8.1128	8.4895	8.7155
		0.990	6.9934	8.2319	1.4226	8.9432	9.2989	9.5122
		0.995	7.8750	9.0775	1.3534	9.7542	10.0925	10.2955
		0.999	9.8205	10.9572	1.2260	11.5702	11.8767	12.0606

(Continued)

Table 5 (continued)

ϑ	δ	q	VaR	TVaR	TV	TVP		
						κ = 0.50	κ = 0.75	κ = 0.90
1.8	1.3	0.900	1.9621	2.5456	0.2755	2.6833	2.7522	2.7935
		0.910	2.0304	2.6067	0.2687	2.7410	2.8082	2.8485
		0.920	2.1059	2.6741	0.2613	2.8047	2.8701	2.9092
		0.930	2.1902	2.7494	0.2531	2.8760	2.9392	2.9772
		0.940	2.2860	2.8348	0.2441	2.9569	3.0179	3.0545
		0.950	2.3970	2.9338	0.2339	3.0507	3.1092	3.1443
		0.960	2.5297	3.0519	0.2224	3.1631	3.2187	3.2520
		0.970	2.6952	3.1995	0.2086	3.3038	3.3560	3.3872
		0.980	2.9185	3.3991	0.1912	3.4947	3.5425	3.5712
		0.990	3.2747	3.7195	0.1670	3.8030	3.8447	3.8698
		0.995	3.6024	4.0173	0.1473	4.0909	4.1277	4.1498
		0.999	4.2776	4.6395	0.1172	4.6981	4.7274	4.7450
	2.1	0.900	2.4385	2.9852	0.2360	3.1032	3.1622	3.1976
		0.910	2.5045	3.0423	0.2294	3.1570	3.2144	3.2488
		0.920	2.5768	3.1051	0.2226	3.2164	3.2721	3.3054
		0.930	2.6569	3.1750	0.2153	3.2826	3.3364	3.3687
		0.940	2.7471	3.2540	0.2074	3.3577	3.4095	3.4406
		0.950	2.8509	3.3452	0.1988	3.4446	3.4943	3.5241
		0.960	2.9739	3.4539	0.1890	3.5484	3.5956	3.6240
		0.970	3.1264	3.5895	0.1778	3.6784	3.7229	3.7496
		0.980	3.3310	3.7729	0.1641	3.8549	3.8960	3.9206
		0.990	3.6570	4.0684	0.1441	4.1404	4.1764	4.1980
		0.995	3.9582	4.3443	0.1297	4.4091	4.4415	4.4610
		0.999	4.5859	4.9280	0.1047	4.9804	5.0066	5.0223

5 Parameter Estimation

Our main goal in this section is to use the ML estimation method to obtain the point and interval estimates of the unknown parameters of the HTPXLD. Assume that $y_1, \ldots, y_n$, a sample of size n, is taken from the HTPXLD specified by the PDF (6). For the vector of parameters $\omega = (\delta, \beta, \vartheta)^T$, the log-likelihood function can be written as

$$\log l^* = n \log\left(\frac{\delta(\delta-1)\vartheta\beta^2}{(1+\beta)^2}\right) + \sum_{i=1}^{n} \log\left(2+\beta+y_i^{\vartheta}\right) - \sum_{i=1}^{n} \beta y_i^{\vartheta} - 2\sum_{i=1}^{n} \log\left[\delta - \left(1+\beta^{\bullet} y_i^{\vartheta}\right) e^{-\beta y_i^{\vartheta}}\right].$$

Regarding the model parameters δ, β, and ϑ, the partial derivatives of $\log l^*$ are obtained, respectively, as follows:

$$\frac{\partial \log l^*}{\partial \delta} = \frac{2n(\delta-1)}{\delta(\delta-1)} - \sum_{i=1}^{n} \frac{2}{\left[\delta - \left(1+\beta^{\bullet} y_i^{\vartheta}\right) e^{-\beta y_i^{\vartheta}}\right]}, \tag{27}$$

$$\frac{\partial \log l^*}{\partial \beta} = \frac{2n}{\beta(1+\beta)} + \sum_{i=1}^{n} \frac{1}{\left(2+\beta+y_i^{\vartheta}\right)} - \sum_{i=1}^{n} y_i^{\vartheta} + \sum_{i=1}^{n} \frac{2y_i^{\vartheta} e^{-\beta y_i^{\vartheta}} \mathrm{M}(y_i, \beta, \vartheta)}{\left[\delta - \left(1+\beta^{\bullet} y_i^{\vartheta}\right) e^{-\beta y_i^{\vartheta}}\right]}, \tag{28}$$

where, $\mathrm{M}(y_i, \beta, \vartheta) = \left[\frac{1-\beta-(1+\beta)^3-\beta(1+\beta)y_i^{\vartheta}}{(1+\beta)^3}\right]$, and

$$\frac{\partial \log l^*}{\partial \vartheta} = \frac{n}{\vartheta} + \sum_{i=1}^{n} \frac{y_i^{\vartheta} \ln y_i}{\left(2+\beta+y_i^{\vartheta}\right)} - \sum_{i=1}^{n} \beta y_i^{\vartheta} \ln y_i - 2\sum_{i=1}^{n} \frac{y^{\vartheta} \ln y_i e^{-\beta y^{\vartheta}} \left[\beta\left(1+\beta^{\bullet} y^{\vartheta}\right) - \beta^{\bullet}\right]}{\left[\delta - \left(1+\beta^{\bullet} y_i^{\vartheta}\right) e^{-\beta y_i^{\vartheta}}\right]}. \tag{29}$$

The non-linear Eqs. (27)–(29) are equated with zero to obtain the ML estimates (MLEs) $\hat{\delta}, \hat{\beta}$, and $\hat{\vartheta}$. As seen, it is difficult to formulate easily, making it challenging to solve them directly for the vector parameter $\omega = (\delta, \beta, \vartheta)^T$. Consequently, iterative techniques are used, such as the Newton-Raphson to get MLEs $\hat{\delta}, \hat{\beta}$, and $\hat{\vartheta}$.

Instead of determining point estimates for the unknown parameters, it would be more helpful to identify a range of values that, with a specified probability, encompass them. These ranges are referred to as interval estimates. To build the parameters CIs, the asymptotic distribution of MLE of $\omega = (\delta, \beta, \vartheta)^T$ will be used, that is

$$(\underline{\hat{\omega}} - \underline{\omega}) \xrightarrow{D} N_3(0, I^{-1}(\underline{\hat{\omega}})),$$

where $\hat{\omega}$ is the MLE of ω and $I^{-1}(\omega)$ is the inverse of the observed information matrix of ω, and it is given by

$$I^{-1}(\hat{\omega}) = \begin{pmatrix} \frac{-\partial^2 \log l^*}{\partial \delta^2} & \frac{-\partial^2 \log l^*}{\partial \delta \partial \beta} & \frac{-\partial^2 \log l^*}{\partial \delta \partial \vartheta} \\ & \frac{-\partial^2 \log l^*}{\partial \beta^2} & \frac{-\partial^2 \log l^*}{\partial \beta \partial \vartheta} \\ & & \frac{-\partial^2 \log l^*}{\partial \vartheta^2} \end{pmatrix}^{-1}_{\hat{\omega}=(\hat{\delta},\hat{\beta},\hat{\vartheta})} = \begin{pmatrix} \hat{\sigma}_{11}^2 & \hat{\sigma}_{12}^2 & \hat{\sigma}_{13}^2 \\ & \hat{\sigma}_{22}^2 & \hat{\sigma}_{23}^2 \\ & & \hat{\sigma}_{33}^2 \end{pmatrix}.$$

Asymptotic normality of the MLEs allows for the construction of the $100(1-\varphi)\%$ asymptotic CIs of and for δ, β, and ϑ, respectively.

$$\hat{\delta} \pm z_{\varphi/2}\hat{\sigma}_{11}, \quad \hat{\beta} \pm z_{\varphi/2}\hat{\sigma}_{22}, \quad \hat{\vartheta} \pm z_{\varphi/2}\hat{\sigma}_{33},$$

where is the upper $\varphi/2$th percentile point of the standard normal distribution.

6 Simulation

This section presents a simulation study to assess the performance of MLEs for the HTPXLD parameters $(\vartheta, \delta, \beta)$. The R package is utilized to compute the mean, relative bias (RBias), bias, mean squared error (MSE), root mean squared error (RMSE), average interval length (AIL) of 95%, and coverage probability (CP) of 95% for the estimated values of ϑ, δ, and β. The simulation process is outlined as follows:

1) Generate 5000 random samples from the HTPXLD with sizes $n = 50, 100, 150, 200, 250, 300, 350$, and 400.

2) Choose parameter values for the simulations as follows: set1 = ($\vartheta = 0.8$, $\delta = 1.5$, $\beta = 0.7$), set2 = ($\vartheta = 0.5$, $\delta = 1.5$, $\beta = 0.7$), set3 = ($\vartheta = 0.5$, $\delta = 1.2$, $\beta = 0.3$), set4 = ($\vartheta = 0.7$, $\delta = 1.6$, $\beta = 0.4$), set5 = ($\vartheta = 1.1$, $\delta = 1.9$, $\beta = 0.7$), and set6 = ($\vartheta = 0.4$, $\delta = 1.7$, $\beta = 0.9$).
3) Compute the MLEs, RBiases, Biases, RMSEs, and MSEs for each sample size and parameter set. Additionally, calculate the AIL and CP at a 95% confidence level for all sample sizes and parameter sets.
4) Present the numerical results in Tables 6–8. The performance of the estimated parameters is analyzed based on complete samples.

Table 6: Simulation values for set1 and set2

n	Parameter	set1 = ($\vartheta = 0.8$, $\delta = 1.5$, $\beta = 0.7$)							set2 = ($\vartheta = 0.5$, $\delta = 1.5$, $\beta = 0.7$)						
		Mean	RBias	Bias	MSE	RMSE	AIL	CP	Mean	RBias	Bias	MSE	RMSE	AIL	CP
50	ϑ	0.9058	0.1322	0.1058	0.0153	0.1239	0.2528	97.04	0.5763	0.1526	0.0763	0.0119	0.1090	0.3054	96.27
	δ	1.7217	0.1478	0.2217	1.3828	1.1759	3.9854	97.87	1.7122	0.1415	0.2122	1.0143	1.0071	3.6420	97.47
	β	0.7313	0.0447	0.0313	0.0239	0.1546	0.5934	96.32	0.7505	0.0721	0.0505	0.0777	0.2787	1.0744	96.68
100	ϑ	0.9045	0.1306	0.1045	0.0137	0.1170	0.2070	96.98	0.5680	0.1360	0.0680	0.0078	0.0882	0.2200	96.33
	δ	1.6086	0.0724	0.1086	0.4165	0.6454	2.4940	97.94	1.5949	0.0633	0.0949	0.3448	0.5872	2.2716	97.80
	β	0.7283	0.0404	0.0283	0.0159	0.1261	0.4817	96.36	0.7440	0.0628	0.0440	0.0447	0.2115	0.8111	96.21
150	ϑ	0.9041	0.1302	0.1041	0.0130	0.1138	0.1801	97.10	0.5659	0.1318	0.0659	0.0059	0.0768	0.1575	96.86
	δ	1.5661	0.0441	0.0661	0.1403	0.3745	1.4451	96.74	1.5604	0.0403	0.0604	0.1134	0.3367	1.2986	96.58
	β	0.7265	0.0379	0.0265	0.0116	0.1079	0.4105	96.50	0.7341	0.0488	0.0341	0.0234	0.1530	0.5847	95.98
200	ϑ	0.9037	0.1296	0.1037	0.0124	0.1114	0.1627	97.08	0.5654	0.1309	0.0654	0.0054	0.0735	0.1276	97.24
	δ	1.5508	0.0338	0.0508	0.1429	0.3781	1.4687	97.80	1.5444	0.0296	0.0444	0.0739	0.2718	1.0511	95.66
	β	0.7260	0.0371	0.0260	0.0099	0.0993	0.3751	96.30	0.7256	0.0366	0.0256	0.0153	0.1236	0.4742	96.46
250	ϑ	0.9035	0.1294	0.1035	0.0121	0.1100	0.1464	97.28	0.5651	0.1302	0.0651	0.0050	0.0710	0.1114	96.98
	δ	1.5342	0.0228	0.0342	0.0580	0.2408	0.9346	95.70	1.5304	0.0203	0.0304	0.0598	0.2446	0.9515	96.36
	β	0.7242	0.0345	0.0242	0.0082	0.0903	0.3412	96.66	0.7242	0.0346	0.0242	0.0098	0.0989	0.3758	96.26
300	ϑ	0.9035	0.1293	0.1035	0.0120	0.1093	0.1363	97.28	0.5650	0.1301	0.0650	0.0049	0.0699	0.1005	97.12
	δ	1.5250	0.0167	0.0250	0.0457	0.2137	0.8319	95.74	1.5223	0.0149	0.0223	0.0389	0.1972	0.7680	95.64
	β	0.7231	0.0329	0.0231	0.0071	0.0840	0.3166	96.78	0.7233	0.0333	0.0233	0.0079	0.0888	0.3359	96.60
350	ϑ	0.9033	0.1292	0.1033	0.0118	0.1086	0.1283	96.90	0.5650	0.1299	0.0650	0.0047	0.0686	0.0853	97.02
	δ	1.5171	0.0114	0.0171	0.0320	0.1788	0.6979	95.46	1.5174	0.0116	0.0174	0.0333	0.1826	0.7125	95.52
	β	0.7218	0.0311	0.0218	0.0062	0.0786	0.2961	97.04	0.7224	0.0320	0.0224	0.0069	0.0829	0.3129	96.72
400	ϑ	0.9032	0.1290	0.1032	0.0116	0.1075	0.1188	97.12	0.5647	0.1295	0.0647	0.0045	0.0674	0.0738	97.24
	δ	1.5132	0.0088	0.0132	0.0264	0.1624	0.6346	95.30	1.5115	0.0077	0.0115	0.0286	0.1690	0.6611	96.16
	β	0.7219	0.0313	0.0219	0.0054	0.0732	0.2738	96.68	0.7218	0.0311	0.0218	0.0063	0.0793	0.2989	96.74

Table 7: Simulation values for set3 and set4

n	Parameter	set3 = ($\vartheta = 0.5$, $\delta = 1.2$, $\beta = 0.3$)							set4 = ($\vartheta = 0.7$, $\delta = 1.6$, $\beta = 0.4$)						
		Mean	RBias	Bias	MSE	RMSE	AIL	CP	Mean	RBias	Bias	MSE	RMSE	AIL	CP
50	ϑ	0.5481	0.0963	0.0481	0.0047	0.0683	0.1901	96.92	0.7960	0.1371	0.0960	0.0185	0.1359	0.3774	95.91
	δ	1.5422	0.2851	0.3422	1.1934	1.0924	3.5758	97.72	1.7977	0.1236	0.1977	1.0371	1.0184	3.7559	98.03
	β	0.3752	0.2508	0.0752	0.0207	0.1438	0.4805	95.26	0.3858	0.0356	0.0142	0.0052	0.0718	0.2782	96.30
100	ϑ	0.5473	0.0947	0.0473	0.0034	0.0586	0.1351	96.88	0.7848	0.1212	0.0848	0.0119	0.1089	0.2678	96.22
	δ	1.3742	0.1452	0.1742	0.1331	0.3648	1.2566	97.02	1.7383	0.0864	0.1383	0.4876	0.6982	2.6831	98.12
	β	0.3620	0.2066	0.0620	0.0108	0.1039	0.3274	96.38	0.3863	0.0342	0.0137	0.0040	0.0634	0.2445	96.34
150	ϑ	0.5462	0.0925	0.0462	0.0029	0.0543	0.1119	97.26	0.7840	0.1199	0.0840	0.0096	0.0981	0.1986	96.98
	δ	1.3517	0.1264	0.1517	0.0708	0.2662	0.8572	96.38	1.6919	0.0574	0.0919	0.1850	0.4301	1.6474	96.58
	β	0.3619	0.2063	0.0619	0.0087	0.0934	0.2741	96.48	0.3864	0.0340	0.0136	0.0033	0.0576	0.2193	96.78

(Continued)

Table 7 (continued)

n	Parameter	set3 = (ϑ = 0.5, δ = 1.2, β = 0.3)							set4 = (ϑ = 0.7, δ = 1.6, β = 0.4)						
		Mean	RBias	Bias	MSE	RMSE	AIL	CP	Mean	RBias	Bias	MSE	RMSE	AIL	CP
200	ϑ	0.5462	0.0924	0.0462	0.0027	0.0523	0.0961	97.14	0.7827	0.1181	0.0827	0.0085	0.0923	0.1610	96.82
	δ	1.3311	0.1092	0.1311	0.0414	0.2036	0.6106	95.78	1.6686	0.0429	0.0686	0.1031	0.3210	1.2295	95.74
	β	0.3590	0.1967	0.0590	0.0071	0.0840	0.2348	96.52	0.3887	0.0281	0.0113	0.0026	0.0515	0.1945	96.88
250	ϑ	0.5461	0.0923	0.0461	0.0025	0.0505	0.0845	96.92	0.7825	0.1178	0.0825	0.0080	0.0893	0.1417	97.10
	δ	1.3259	0.1049	0.1259	0.0331	0.1819	0.5145	95.72	1.6476	0.0298	0.0476	0.0757	0.2752	1.0626	95.14
	β	0.3589	0.1965	0.0589	0.0063	0.0794	0.2081	96.58	0.3891	0.0272	0.0109	0.0024	0.0489	0.1818	96.74
300	ϑ	0.5460	0.0919	0.0460	0.0025	0.0497	0.0784	97.02	0.7822	0.1174	0.0822	0.0076	0.0869	0.1144	97.08
	δ	1.3221	0.1018	0.1221	0.0284	0.1685	0.4550	95.52	1.6443	0.0277	0.0443	0.0638	0.2526	0.9750	95.96
	β	0.3587	0.1956	0.0587	0.0058	0.0759	0.1889	96.56	0.3915	0.0212	0.0085	0.0021	0.0457	0.1690	97.02
350	ϑ	0.5459	0.0918	0.0459	0.0025	0.0496	0.0725	97.36	0.7819	0.1170	0.0819	0.0074	0.0861	0.1008	96.94
	δ	1.3152	0.0960	0.1152	0.0247	0.1571	0.4190	95.76	1.6416	0.0260	0.0416	0.0581	0.2411	0.9310	96.38
	β	0.3569	0.1896	0.0569	0.0052	0.0724	0.1772	96.72	0.3970	0.0075	0.0030	0.0019	0.0437	0.1620	97.22
400	ϑ	0.5456	0.0912	0.0456	0.0024	0.0493	0.0676	97.66	0.7812	0.1160	0.0812	0.0072	0.0851	0.0904	97.08
	δ	1.3123	0.0936	0.1123	0.0217	0.1472	0.3730	95.70	1.6320	0.0200	0.0320	0.0460	0.2145	0.8314	95.84
	β	0.3566	0.1886	0.0566	0.0049	0.0698	0.1632	96.70	0.4015	0.0038	0.0015	0.0018	0.0420	0.1533	97.08

Table 8: Simulation values for set5 and set6

n	Parameter	set5 = (ϑ = 1.1, δ = 1.9, β = 0.7)							set6 = (ϑ = 0.4, δ = 1.7, β = 0.9)						
		Mean	RBias	Bias	MSE	RMSE	AIL	CP	Mean	RBias	Bias	MSE	RMSE	AIL	CP
50	ϑ	1.2640	0.1491	0.1640	0.0326	0.1805	0.2948	96.72	0.4733	0.1833	0.0733	0.0094	0.0971	0.2493	95.56
	δ	1.7362	0.0862	0.1638	1.8461	1.3587	4.6438	98.13	1.5771	0.0723	0.1229	0.5111	0.7149	2.8026	97.62
	β	0.6544	0.0651	0.0456	0.0142	0.1193	0.4416	96.66	0.8806	0.0216	0.0194	0.0199	0.1410	0.5505	96.34
100	ϑ	1.2660	0.1509	0.1660	0.0318	0.1783	0.2552	97.26	0.4664	0.1661	0.0664	0.0066	0.0810	0.1818	96.15
	δ	1.7464	0.0809	0.1536	1.3245	1.1509	4.1466	98.58	1.5823	0.0692	0.1177	0.1510	0.3886	1.5058	96.08
	β	0.6550	0.0643	0.0450	0.0117	0.1083	0.3873	96.68	0.8814	0.0207	0.0186	0.0149	0.1222	0.4762	96.64
150	ϑ	1.2642	0.1492	0.1642	0.0303	0.1740	0.2262	97.12	0.4640	0.1599	0.0640	0.0052	0.0719	0.1283	96.92
	δ	1.7562	0.0757	0.1438	0.4419	0.6648	2.5872	97.70	1.5854	0.0674	0.1146	0.1199	0.3463	1.3183	96.58
	β	0.6555	0.0636	0.0445	0.0096	0.0981	0.3429	96.70	0.8817	0.0204	0.0183	0.0124	0.1113	0.4311	96.70
200	ϑ	1.2638	0.1489	0.1638	0.0296	0.1720	0.2056	97.28	0.4631	0.1579	0.0631	0.0047	0.0687	0.1057	96.82
	δ	1.7721	0.0673	0.1279	0.1947	0.4413	1.6687	96.18	1.5970	0.0606	0.1030	0.0742	0.2723	0.9929	95.54
	β	0.6557	0.0633	0.0443	0.0083	0.0909	0.3086	96.82	0.8827	0.0192	0.0173	0.0098	0.0989	0.3819	96.80
250	ϑ	1.2627	0.1479	0.1627	0.0289	0.1701	0.1953	97.04	0.4627	0.1568	0.0627	0.0045	0.0670	0.0924	97.00
	δ	1.7836	0.0613	0.1164	0.1748	0.4181	1.5604	96.56	1.5999	0.0589	0.1001	0.0657	0.2564	0.9204	95.74
	β	0.6607	0.0561	0.0393	0.0074	0.0858	0.2864	96.92	0.8829	0.0190	0.0171	0.0088	0.0941	0.3633	97.20
300	ϑ	1.2629	0.1481	0.1629	0.0287	0.1693	0.1802	96.84	0.4625	0.1563	0.0625	0.0044	0.0660	0.0823	97.22
	δ	1.9858	0.0452	0.0858	0.1164	0.3412	1.2132	95.60	1.6174	0.0486	0.0826	0.0591	0.2431	0.8406	96.08
	β	0.6656	0.0491	0.0344	0.0068	0.0826	0.2695	97.08	0.8839	0.0179	0.0161	0.0078	0.0881	0.3367	96.92
350	ϑ	1.2640	0.1491	0.1640	0.0288	0.1697	0.1709	96.94	0.4625	0.1563	0.0625	0.0043	0.0653	0.0738	97.08
	δ	1.8199	0.0421	0.0801	0.1117	0.3343	1.1639	95.64	1.6412	0.0346	0.0588	0.0527	0.2297	0.7731	95.84
	β	0.6675	0.0464	0.0325	0.0064	0.0802	0.2551	96.72	0.8865	0.0150	0.0135	0.0069	0.0829	0.3169	97.08
400	ϑ	1.2636	0.1487	0.1636	0.0284	0.1686	0.1596	97.02	0.4622	0.1554	0.0622	0.0042	0.0646	0.0650	97.14
	δ	1.8908	0.0048	0.0092	0.0963	0.3103	1.0332	95.52	1.7009	0.0005	0.0009	0.0451	0.2125	0.6796	95.76
	β	0.6683	0.0453	0.0317	0.0060	0.0776	0.2406	96.88	0.8877	0.0137	0.0123	0.0059	0.0771	0.2934	97.08

The results show in Tables 6–8 that bias, MSE, and RMSE all significantly decrease with increasing sample size (n). Furthermore, higher sample sizes increase CP and AIL, producing more accurate and trustworthy estimates and confidence ranges.

- Greater sample sizes lead to improvements in MSE. As the sample size increases, the parameter estimates converge closer to the real values, indicating that the MLEs are becoming more exact, as indicated by lower MSE values.
- As the sample size grows, the CP gets better, indicating that the CIs created for the parameter estimates get more trustworthy. The robustness of the estimates is improved by higher CP values, which indicate a higher probability that the intervals include the genuine parameter values.
- As the sample size grows, the values of AIL become lower.

7 Applications

This section demonstrates the applicability of the HTPXLD in fitting real-world data by evaluating it against three actual datasets. The HTPXLD is compared with several alternative models, including XLD [1], Lindley (LD) [51], exponentiated generalized XLD (EGXLD) [52], power exponentiated LD (PELD) [53], Kumaraswamy LD (KLD) [54], Weibull power LD (WPLD) [15], exponentiated generalized power LD (EGLD) [55], power LD (PLD) [56], Weibull LD (WLD) [57], extended LD (EXLD) [58], and PXLD.

We use nine well-established goodness-of-fit measures to compare these models, including the Kolmogorov-Smirnov ($\mathfrak{R}_6$) statistic, its p-value ($\mathfrak{R}_7$), Anderson-Darling statistics ($\mathfrak{R}_{10}$), its p-value ($\mathfrak{R}_{11}$), the Hannan-Quinn Information Criterion ($\mathfrak{R}_5$), Akaike Information Criterion ($\mathfrak{R}_2$), Bayesian Information Criterion ($\mathfrak{R}_3$), Consistent $\mathfrak{R}_2$ ($\mathfrak{R}_4$), Cramér-von Mises statistic ($\mathfrak{R}_8$), and its p-value ($\mathfrak{R}_9$). The optimal model is identified based on the highest values for $\mathfrak{R}_7$, $\mathfrak{R}_{11}$, and $\mathfrak{R}_9$, and the lowest values for $\mathfrak{R}_6$, $\mathfrak{R}_{10}$, $\mathfrak{R}_8$, $\mathfrak{R}_5$, $\mathfrak{R}_2$, $\mathfrak{R}_4$, and $\mathfrak{R}_3$.

7.1 The First Dataset

The first dataset consists of repair times for an airborne communication transceiver, provided by [59]. The recorded times are: 0.50, 0.60, 0.60, 0.70, 0.70, 0.70, 0.80, 0.80, 1.00, 1.00, 1.00, 1.00, 1.10, 1.30, 1.50, 1.50, 1.50, 1.50, 2.00, 2.00, 2.20, 2.50, 2.70, 3.00, 3.00, 3.30, 4.00, 4.00, 4.50, 4.70, 5.00, 5.40, 5.40, 7.00, 7.50, 8.80, 9.00, 10.20, 22.00, 24.50. Table 9 displays the results of the descriptive analysis for this dataset.

Table 9: Descriptive statistics for the first dataset

n	Mean	Median	σ^2	σ	κ_1	κ_2	Range	Minimum	Maximum	Sum
40	4.0125	2.1000	26.6801	5.1653	2.7171	10.5433	24.0000	0.5000	24,5000	160.5000

For the first dataset, Table 10 presents the MLEs along with their standard errors (SEs). Table 11 provides the numerical values for the $\mathfrak{R}_6$ statistic, its $\mathfrak{R}_7$, $\mathfrak{R}_{10}$, its $\mathfrak{R}_{11}$, $\mathfrak{R}_8$, its $\mathfrak{R}_9$, as well as the $\mathfrak{R}_2$, $\mathfrak{R}_3$, $\mathfrak{R}_4$, and $\mathfrak{R}_5$ statistics. Fig. 3 includes the histogram, violin plot, QQ (quantile-quantile) plot, box plot with strip chart, and TTT (total time in test) plot. The estimated PDFs of competing models for the first dataset are shown in Fig. 4, while Fig. 5 displays the estimated CDFs of the competitive models. Additionally, Fig. 6 illustrates the PP plots of the competing models. Figs. 4–6 demonstrate the fit of our distribution to the actual data.

Table 10: Estimates values and SEs for all models applied to the first dataset

Models	$\hat{\delta}$	$\hat{\beta}$	$\hat{\vartheta}$	$\hat{\eta}$	SE($\hat{\delta}$)	SE($\hat{\beta}$)	SE($\hat{\vartheta}$)	SE($\hat{\eta}$)
HTPXLD	1.0281	0.0584	1.2010		0.0473	0.0520	0.1296	
XLD	0.3811				0.0442			
PXLD	0.4762	0.8547			0.0820	0.0861		

(Continued)

Table 10 (continued)

Models	$\hat{\delta}$	$\hat{\beta}$	$\hat{\vartheta}$	$\hat{\eta}$	SE($\hat{\delta}$)	SE($\hat{\beta}$)	SE($\hat{\vartheta}$)	SE($\hat{\eta}$)
LD	0.4242				0.0485			
PLD	0.7989	0.5867			0.0822	0.0994		
EGXLD	0.1804	1.5616	1.0488		0.0384	0.0026	0.2279	
PELD	0.9251	0.0353	0.2217		0.1698	0.0545	0.0797	
KLD	1.5614	1.4776	0.2033		0.0035	0.0341	0.0322	
WPLD	0.0052	1.0898	71.8390	120.0244	0.0009	0.0214	164.8468	13.8702
EGLD	1.5752	0.1798	0.9358		0.0035	0.0393	0.1985	
WLD	0.9604	0.2546	0.0000		0.1089	0.0446	0.0541	
EXLD	0.0081	1.0682	0.0806		4.3109	0.2829	0.0931	

Table 11: Fitting measures values for the first data set

Models	$\mathfrak{R}_1$	$\mathfrak{R}_2$	$\mathfrak{R}_3$	$\mathfrak{R}_4$	$\mathfrak{R}_5$	$\mathfrak{R}_6$	$\mathfrak{R}_7$	$\mathfrak{R}_8$	$\mathfrak{R}_9$	$\mathfrak{R}_{10}$	$\mathfrak{R}_{11}$
HTPXLD	185.8189	191.8189	196.8855	192.4856	193.6508	0.1158	0.6566	0.0751	0.7234	0.6135	0.6342
XLD	195.0261	197.0261	198.7150	197.1313	197.6367	0.1838	0.1341	0.2847	0.1492	1.7324	0.1298
PXLD	192.2416	196.2416	199.6194	196.5660	197.4629	0.1387	0.4253	0.1399	0.4234	1.0735	0.3205
LD	197.5826	199.5826	201.2715	199.6879	200.1933	0.2157	0.0484	0.4120	0.0667	2.4386	0.0537
PLD	191.8854	195.8854	199.2631	196.2097	197.1067	0.1345	0.4639	0.1366	0.4345	1.0387	0.3371
EGXLD	191.0672	197.0672	202.1338	197.7338	198.8991	0.1596	0.2600	0.2052	0.2582	1.2995	0.2324
PELD	256.1107	262.1107	267.1774	262.7774	263.9427	0.1425	0.3909	0.1187	0.5026	0.8830	0.4242
KLD	191.5231	197.5231	202.5898	198.1898	199.3551	0.2101	0.0585	0.3710	0.0859	2.1543	0.0760
WPLD	191.1065	199.1065	205.8621	200.2494	201.5491	0.1296	0.5123	0.1366	0.4348	1.0264	0.3432
EGLD	192.0077	198.0077	203.0743	198.6744	199.8396	0.1615	0.2479	0.2150	0.2405	1.3484	0.2171
WLD	191.0227	197.0227	202.0894	197.6894	198.8547	0.1290	0.5181	0.1359	0.4371	1.0212	0.3459
EXLD	189.1611	195.1611	200.2278	195.8278	196.9931	0.1328	0.4808	0.1000	0.5870	0.8413	0.4514

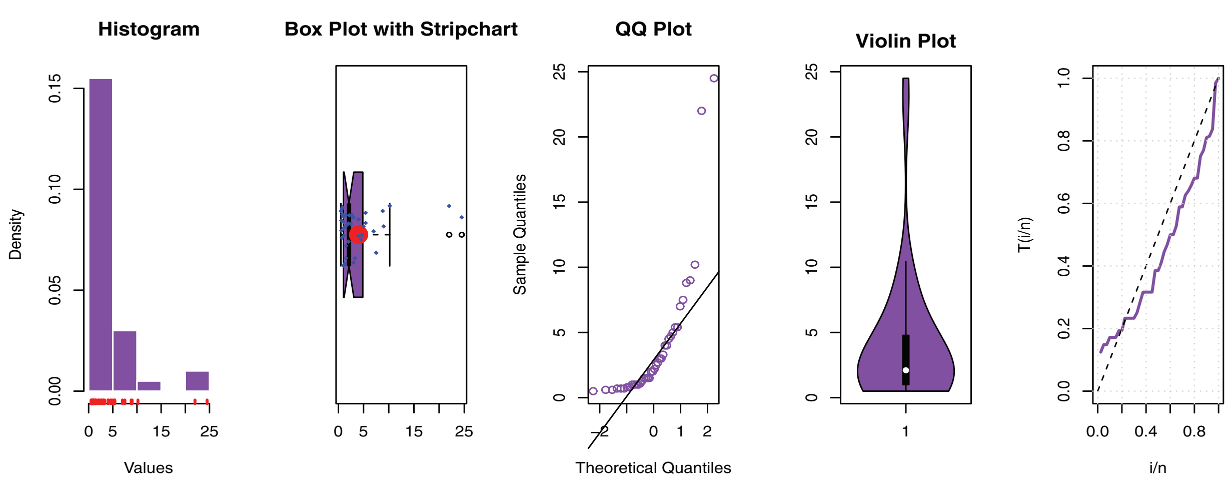

Figure 3: Some basic non-parametric plots for the first dataset

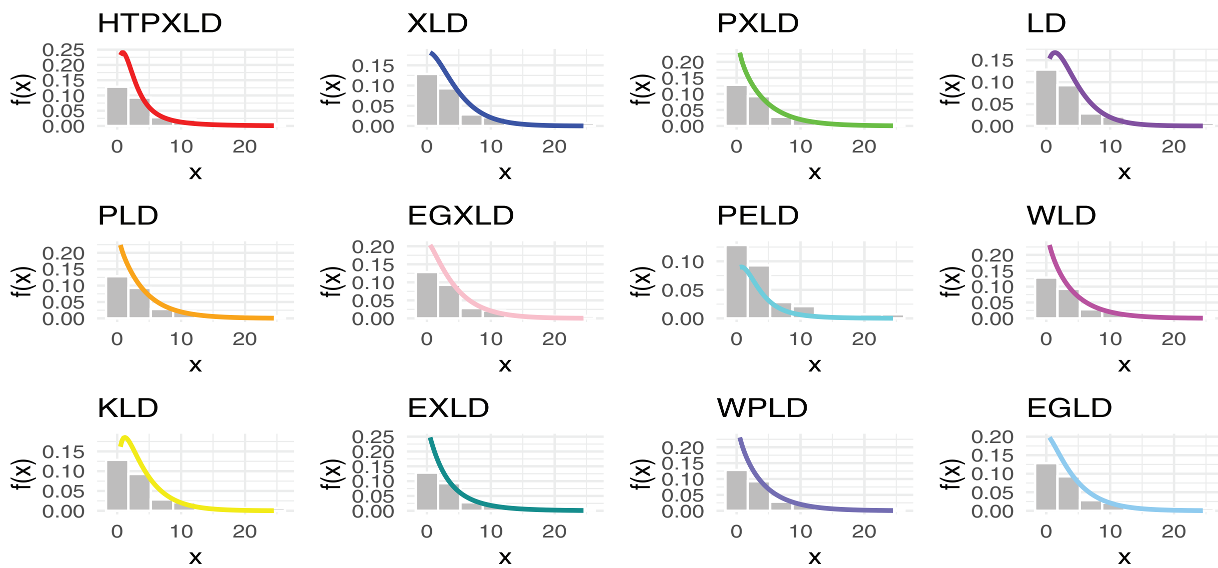

Figure 4: Estimated PDFs for the competing models for the first dataset

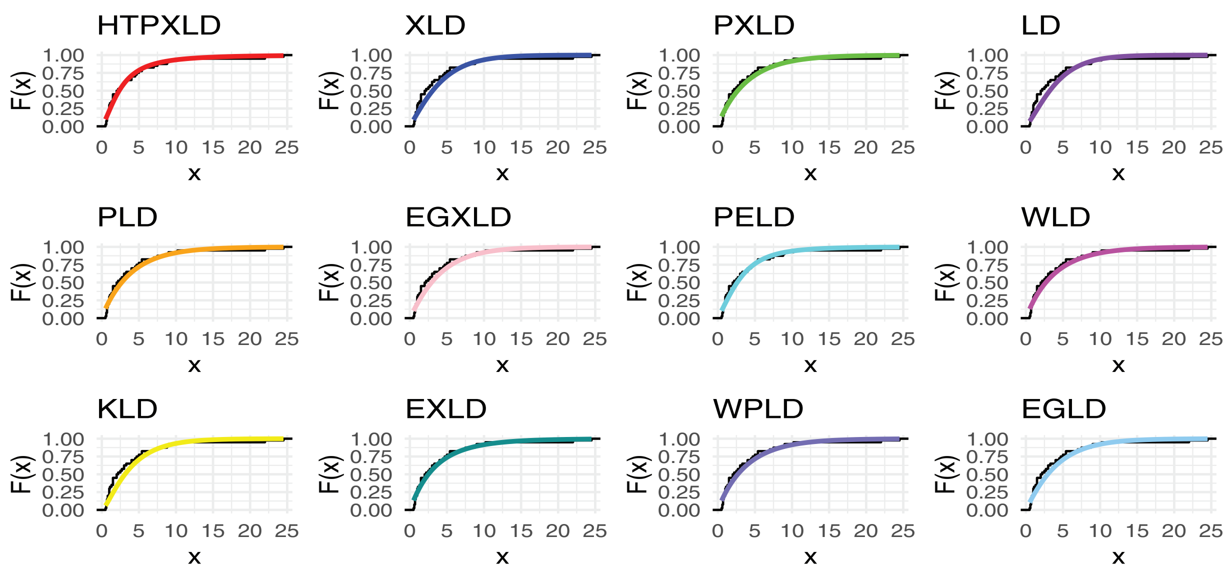

Figure 5: Estimated CDFs for the competing models for the first dataset

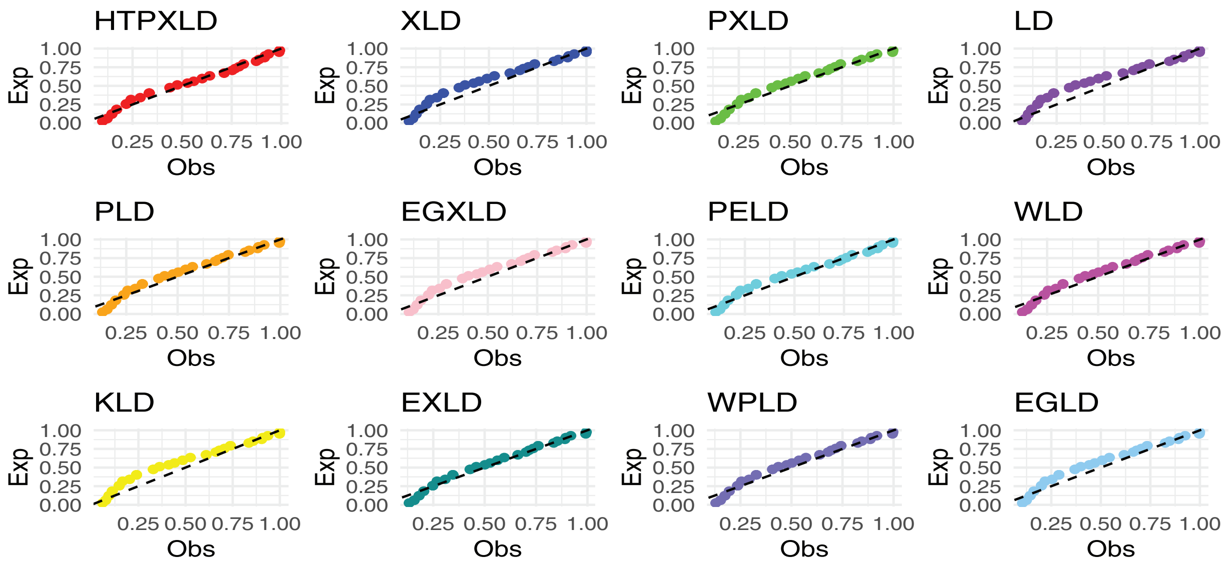

Figure 6: PP plots of competing models for the first dataset

7.2 The Second Dataset

The data set provided by [60] shows the monthly remission periods of 128 individuals with bladder cancer who were selected at random. the data set that we work with is 0.08, 2.09, 3.48, 4.87, 6.94, 8.66, 13.11, 23.63, 0.2, 2.23, 3.52, 4.98, 6.97, 9.02, 13.29, 0.4, 2.26, 3.57, 5.06, 7.09, 9.22, 13.8, 25.74, 0.5, 2.46, 3.64, 5.09, 7.26, 9.47, 14.24, 25.82, 0.51, 2.54, 3.7, 5.17, 7.28, 9.74, 14.76, 6.31, 0.81, 2.62, 3.82, 5.32, 7.32, 10.06, 14.77, 32.15, 2.64, 3.88, 5.32, 7.39, 10.34, 14.83, 34.26, 0.9, 2.69, 4.18, 5.34, 7.59, 10.66, 15.96, 36.66, 1.05, 2.69, 4.23, 5.41, 7.62, 10.75, 16.62, 43.01, 1.19, 2.75, 4.26, 5.41, 7.63, 17.12, 46.12, 1.26, 2.83, 4.33, 5.49, 7.66, 11.25, 17.14, 79.05, 1.35, 2.87, 5.62, 7.87, 11.64, 17.36, 1.4, 3.02, 4.34, 5.71, 7.93, 11.79, 18.1, 1.46, 4.4, 5.85, 8.26, 11.98, 19.13, 1.76, 3.25, 4.5, 6.25, 8.37, 12.02, 2.02, 3.31, 4.51, 6.54, 8.53, 12.03, 20.28, 2.02, 3.36, 6.76, 12.07, 21.73, 2.07, 3.36, 6.93, 8.65, 12.63, 22.69.

Table 12 displays the results of the descriptive analysis for this dataset.

Table 12: Descriptive statistics for the second dataset

n	Mean	Median	σ^2	σ	κ_1	κ_2	Range	Minimum	Maximum	Sum
128	9.2094	6.2800	108.2132	10.40256	3.3987	19.3942	78.9700	0.0800	79.0500	1178.8000

For the second dataset, Table 13 presents the MLEs along with their SEs. Table 14 provides the numerical values for the $\mathfrak{R}_6$ statistic, its $\mathfrak{R}_7$, $\mathfrak{R}_{10}$, its $\mathfrak{R}_{11}$, $\mathfrak{R}_8$, its $\mathfrak{R}_9$, as well as the $\mathfrak{R}_2$, $\mathfrak{R}_3$, $\mathfrak{R}_4$, and $\mathfrak{R}_5$ statistics. Fig. 7 includes the histogram, violin plot, QQ plot, box plot with strip chart, and TTT plot. The estimated PDFs of competing models for the second dataset are shown in Fig. 8, while Fig. 9 displays the estimated CDFs of the competitive models. Additionally, Fig. 10 illustrates the PP plots of the competing models. Figs. 8–10 demonstrated the fit of our distribution to the actual data.

Table 13: Estimates values and SEs for all models applied to the second data set

Models	$\hat{\delta}$	$\hat{\beta}$	$\hat{\vartheta}$	$\hat{\eta}$	SE($\hat{\delta}$)	SE($\hat{\beta}$)	SE($\hat{\vartheta}$)	SE($\hat{\eta}$)
HTPXLD	1.0376	0.0297	1.1444		0.0437	0.0184	0.0662	
XLD	0.1859				0.0118			
PXLD	0.2422	0.8835			0.0298	0.0478		
LD	0.1992				0.0125			
PLD	0.8346	0.2950			0.0473	0.0370		
EGXLD	0.2916	0.4800	1.0244		0.0345	0.0056	0.1218	
PELD	0.8743	0.0224	0.0876		0.0939	0.0301	0.0262	
KLD	0.5015	0.9518	0.2795		0.0028	0.1661	0.0273	
WPLD	0.0081	1.0747	46.7070	84.8577	0.0020	0.0673	395.3561	17.2771
EGLD	0.4873	0.2821	0.8991		0.0050	0.0344	0.1042	
WLD	1.0514	0.1062	0.0002		0.0675	0.0094	0.0159	
EXLD	0.0022	1.2330	0.0423		4.2883	0.2490	0.0547	

Table 14: Fitting measures values for the second data set

Models	$\mathfrak{R}_1$	$\mathfrak{R}_2$	$\mathfrak{R}_3$	$\mathfrak{R}_4$	$\mathfrak{R}_5$	$\mathfrak{R}_6$	$\mathfrak{R}_7$	$\mathfrak{R}_8$	$\mathfrak{R}_9$	$\mathfrak{R}_{10}$	$\mathfrak{R}_{11}$
HTPXLD	812.8935	818.8935	827.4496	819.0871	822.3699	0.0281	1.0000	0.0112	1.0000	0.0778	1.0000
XLD	829.9418	831.9418	834.7939	831.9736	833.1006	0.1017	0.1415	0.3348	0.1081	1.7385	0.1286
PXLD	824.1349	828.1349	833.8390	828.2309	830.4525	0.0744	0.4785	0.1641	0.3498	1.0405	0.3366
LD	833.7925	835.7925	838.6445	835.8242	836.9513	0.1114	0.0834	0.4851	0.0433	2.6005	0.0440
PLD	822.1099	826.1099	831.8139	826.2059	828.4274	0.0702	0.5538	0.1350	0.4393	0.8517	0.4449
EGXLD	823.7563	829.7563	838.3124	829.9498	833.2327	0.0852	0.3104	0.1902	0.2875	1.0352	0.3392
PELD	1028.9585	1034.9585	1043.5146	1035.1521	1038.4349	0.0447	0.9604	0.0383	0.9421	0.2559	0.9671
KLD	823.5787	829.5787	838.1347	829.7722	833.0550	0.1003	0.1518	0.3078	0.1285	1.5033	0.1757
WPLD	824.0243	832.0243	843.4324	832.3495	836.6595	0.0725	0.5117	0.1696	0.3354	1.0694	0.3227
EGLD	823.1934	829.1934	837.7495	829.3870	832.6698	0.0823	0.3514	0.1742	0.3238	0.9652	0.3759
WLD	823.7849	829.7849	838.3410	829.9785	833.2613	0.0721	0.5192	0.1664	0.3436	1.0484	0.3327
EXLD	822.7917	828.7917	837.3478	828.9852	832.2681	0.0922	0.2265	0.2100	0.2490	1.3555	0.2151

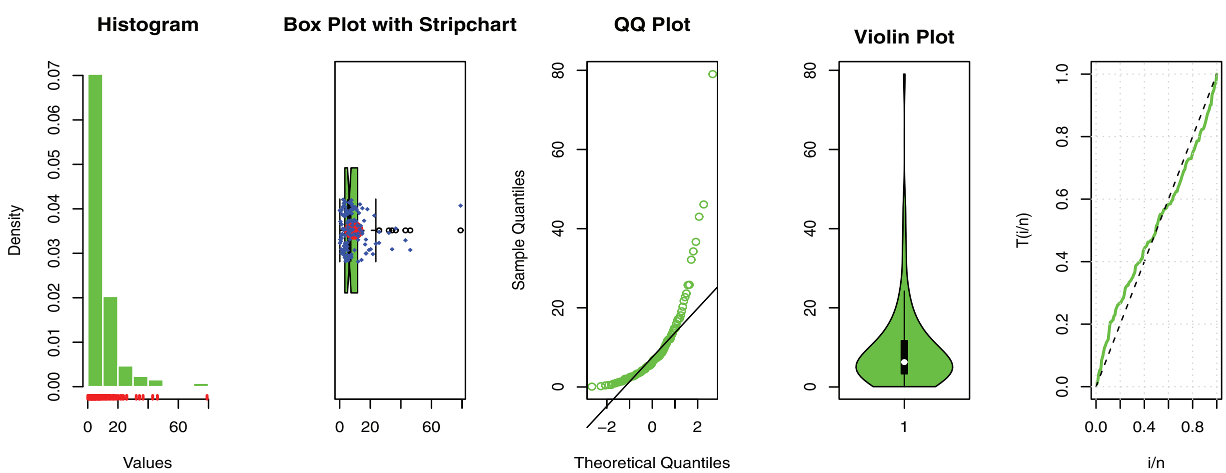

Figure 7: Some basic non-parametric plots for the second dataset

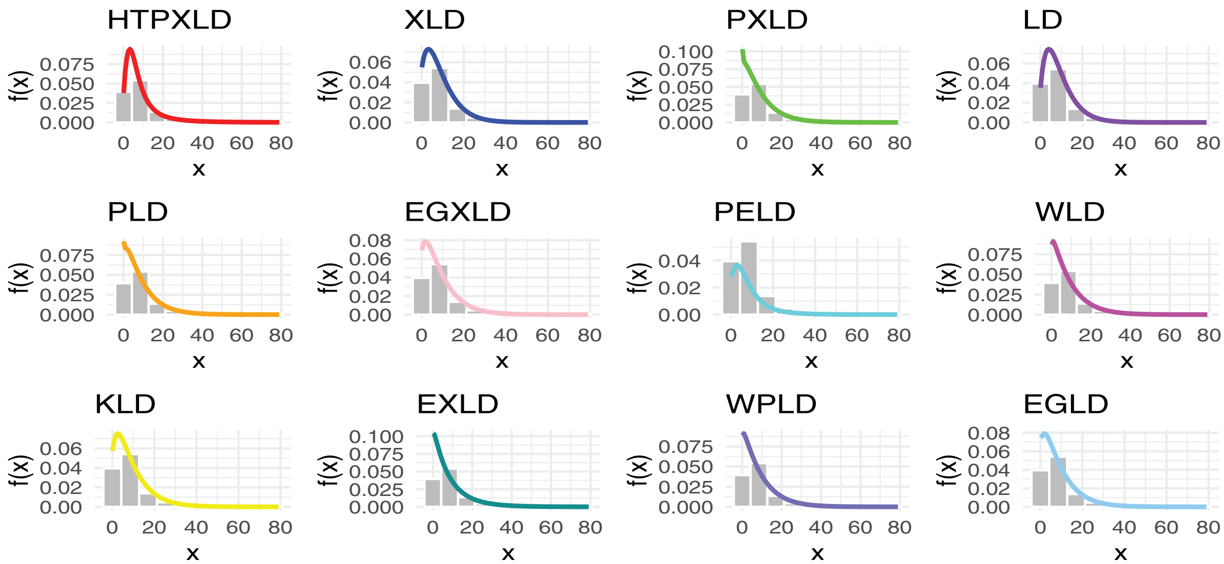

Figure 8: Estimated PDFs for the competing models for the second dataset

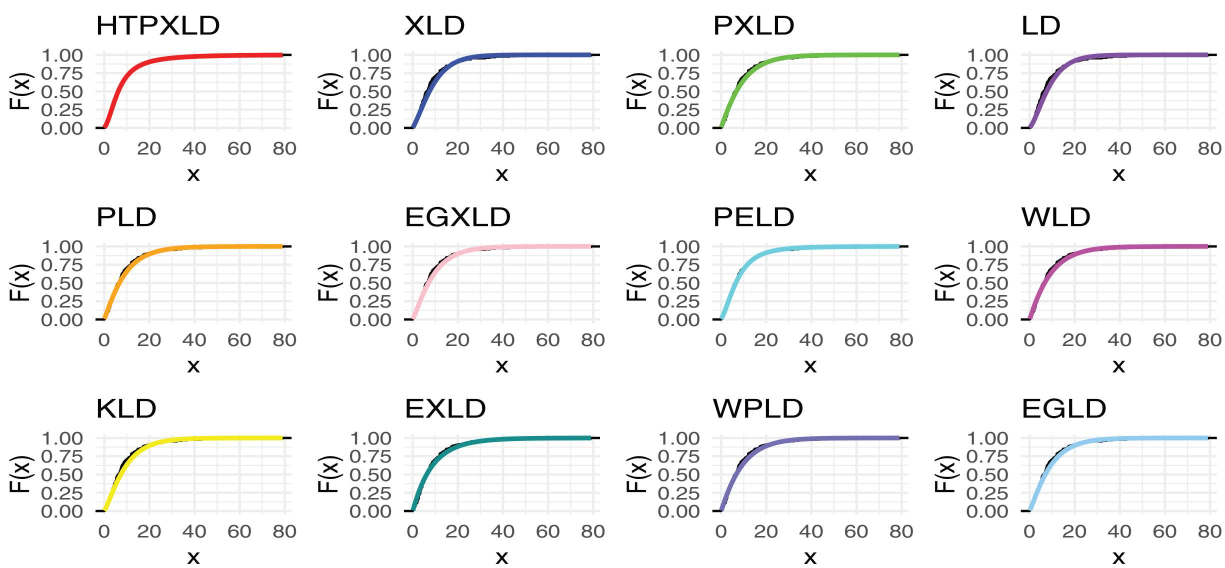

Figure 9: Estimated CDFs for the competing models for the second dataset

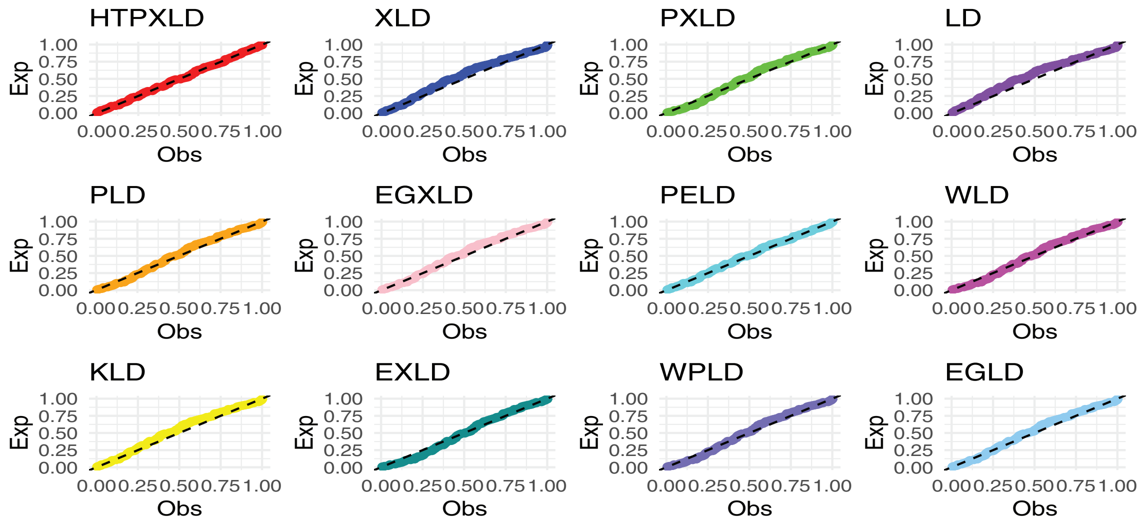

Figure 10: Estimated CDFs for the competing models for the second dataset

7.3 The Third Dataset

The third data set represents values for the inflation rate in several countries that were recorded in June 2024. The term "inflation rate" describes how prices for products and services vary over time. The electronic address from which it was taken is as follows: https://tradingeconomics.com/ (accessed on 07 February 2025). The data set is reported in Table 15. Table 16 displays the results of the descriptive analysis for this dataset.

Table 15: Inflation rate recorded in June 2024

Country	Inflation rate %	Country	Inflation rate %	Country	Inflation rate %	Country	Inflation rate %
Australia	3.60	Germany	2.20	Netherlands	3.20	Spain	3.40
Brazil	3.93	India	4.75	Russia	8.30	Switzerland	1.30
Canada	2.90	Indonesia	2.51	United Kingdom	2.00	Saudi Arabia	1.60
China	0.30	Italy	0.80	Singapore	3.10	United States	3.30
Euro Area	2.50	South Africa	5.20	Japan	2.80		
France	2.20	Mexico	4.69	South Korea	2.40		

Table 16: Descriptive statistics for the third dataset

n	Mean	Median	σ^2	σ	κ_1	κ_2	Range	Minimum	Maximum	Sum
22	3.0445	2.8500	2.8805	1.6972	1.2190	5.4068	8.0000	0.3000	8.3000	66.9800

For the third dataset, Table 17 presents the MLEs along with their SEs. Table 18 provides the numerical values for the $\mathfrak{R}_6$ statistic, its $\mathfrak{R}_7$, $\mathfrak{R}_{10}$, its $\mathfrak{R}_{11}$, $\mathfrak{R}_8$, its $\mathfrak{R}_9$, as well as the $\mathfrak{R}_2$, $\mathfrak{R}_3$, $\mathfrak{R}_4$, and $\mathfrak{R}_5$ statistics. Fig. 11 includes the histogram, violin plot, QQ plot, box plot with strip chart, and TTT plot. The estimated PDFs of competing models for the third dataset are shown in Fig. 12, while Fig. 13 displays the estimated CDFs of the competitive models. Additionally, Fig. 14 illustrates the PP plots of the competing models. Figs. 12–14 demonstrate the fit of our distribution to the actual data.

From the numerical values in Tables 11, 14, and 18 the HTPXLD is better than XLD, LD, EGXLD, PELD, KLD, WPLD, EGLD, PLD, WLD, EXLD, and PXLD for the three datasets.

Table 17: Estimates values and SEs for all models applied to the third data set

Models	$\hat{\delta}$	$\hat{\beta}$	$\hat{\vartheta}$	$\hat{\eta}$	SE($\hat{\delta}$)	SE($\hat{\beta}$)	SE($\hat{\vartheta}$)	SE($\hat{\eta}$)
HTPXLD	1.0698	0.0401	2.0517		0.2073	0.0648	0.3153	
XLD	0.4758				0.0756			
PXLD	0.2407	1.6102			0.0728	0.2161		
LD	0.5414				0.0843			
PLD	1.5161	0.2948			0.2132	0.0908		
EGXLD	59.2893	0.0505	2.0251		243.7637	0.1162	0.7654	
PELD	1.3771	30.4806	0.9934		1.2941	95.0480	0.1759	
KLD	0.3463	1.7807	4.1649		0.4822	0.8894	9.8057	
WPLD	0.0200	1.0710	13.3755	61.8533	0.0187	0.0923	23.0746	55.0031
EGLD	4.6251	0.1411	3.0186		0.0026	0.0299	1.0152	
WLD	1.9006	0.2919	0.0000		0.3030	0.0345	0.7661	
EXLD	0.0797	1.8331	0.3009		0.6872	0.6462	0.0880	

Table 18: Fitting measures values for the third data set

Models	$\mathfrak{R}_1$	$\mathfrak{R}_2$	$\mathfrak{R}_3$	$\mathfrak{R}_4$	$\mathfrak{R}_5$	$\mathfrak{R}_6$	$\mathfrak{R}_7$	$\mathfrak{R}_8$	$\mathfrak{R}_9$	$\mathfrak{R}_{10}$	$\mathfrak{R}_{11}$
HTPXLD	80.3785	86.3785	89.6516	87.7118	87.1495	0.0968	0.9861	0.0290	0.9817	0.2310	0.9795
XLD	90.0141	92.0141	93.1051	92.2141	92.2711	0.2634	0.0945	0.3685	0.0869	1.8797	0.1076
PXLD	84.3294	88.3294	90.5114	88.9609	88.8434	0.1119	0.9458	0.0541	0.8563	0.3470	0.8982
LD	87.6773	89.6773	90.7684	89.8773	89.9343	0.2417	0.1531	0.2938	0.1405	1.5116	0.1739
PLD	83.7147	87.7147	89.8968	88.3463	88.2287	0.1112	0.9483	0.0499	0.8816	0.3238	0.9184
EGXLD	81.2359	87.2359	90.5090	88.5692	88.0069	0.1206	0.9060	0.0519	0.8695	0.3383	0.9059
PELD	116.9745	122.9745	126.2476	124.3078	123.7455	0.0980	0.9841	0.0324	0.9704	0.2461	0.9723
KLD	81.1021	87.1021	90.3752	88.4354	87.8731	0.1176	0.9211	0.0487	0.8888	0.3199	0.9217
WPLD	81.5916	89.5916	93.9558	91.9445	90.6197	0.1234	0.8913	0.0610	0.8127	0.3839	0.8632
EGLD	81.6568	87.6568	90.9299	88.9901	88.4278	0.1509	0.6981	0.0794	0.7000	0.4771	0.7685
WLD	81.5766	87.5766	90.8497	88.9099	88.3476	0.1229	0.8937	0.0603	0.8170	0.3811	0.8660
EXLD	81.5617	87.5617	90.8348	88.8950	88.3328	0.1265	0.8732	0.0610	0.8129	0.3907	0.8565

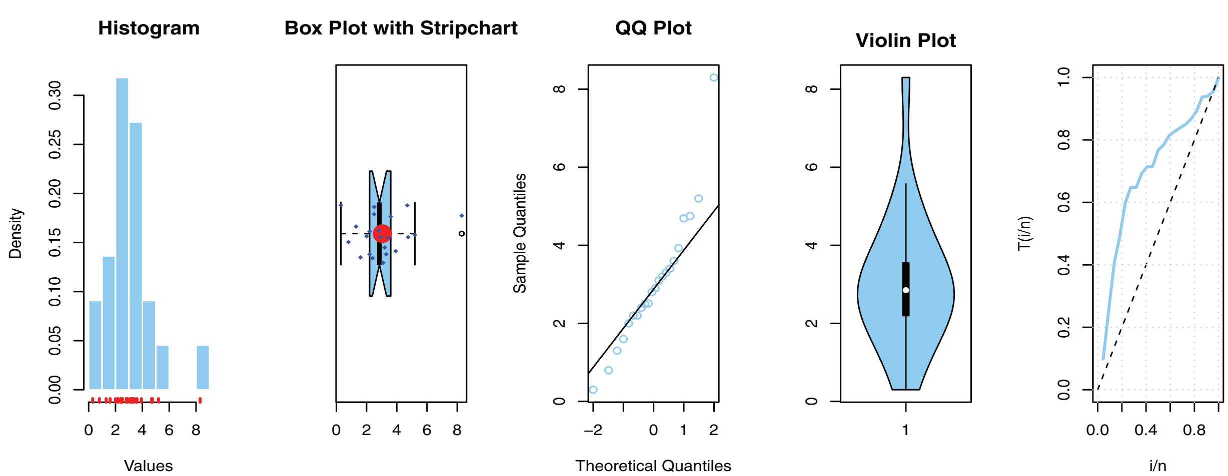

Figure 11: Some basic non-parametric plots for the third dataset

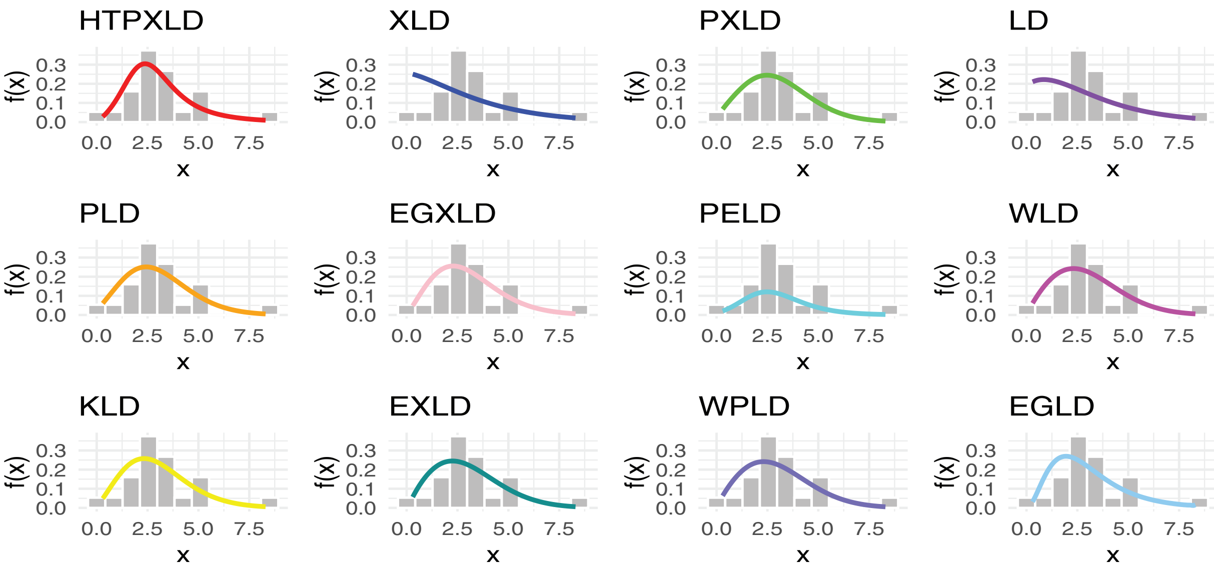

Figure 12: Estimated PDFs for the competing models for the third dataset

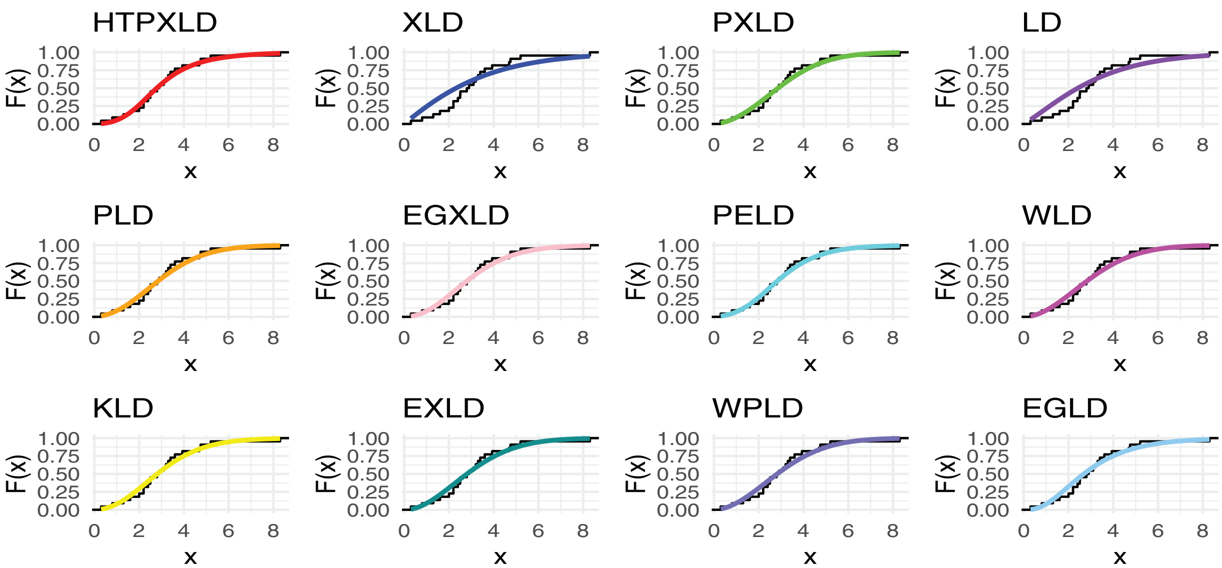

Figure 13: Estimated CDFs for the competing models for the third dataset

The actuarial measures VaR, TVaR, TV, and TVP of the HTPXLD, PXLD, PLD, EGXLD, WLD, KLD, EXLD, and WPLD are computed and compared using the third data set in the following. Tables 19 and 20 present the numerical findings.

We find that for different significance levels q and different values of ω, the HTPXLD model has greater values of the risk measures VaR, TVaR, TV, and TVP from Tables 19 and 20 and the Figs. 15 and 16. This suggests that compared to the PXLD, PLD, EGXLD, WLD, KLD, EXLD, and WPLD, the HTPXLD has a heavier tail.

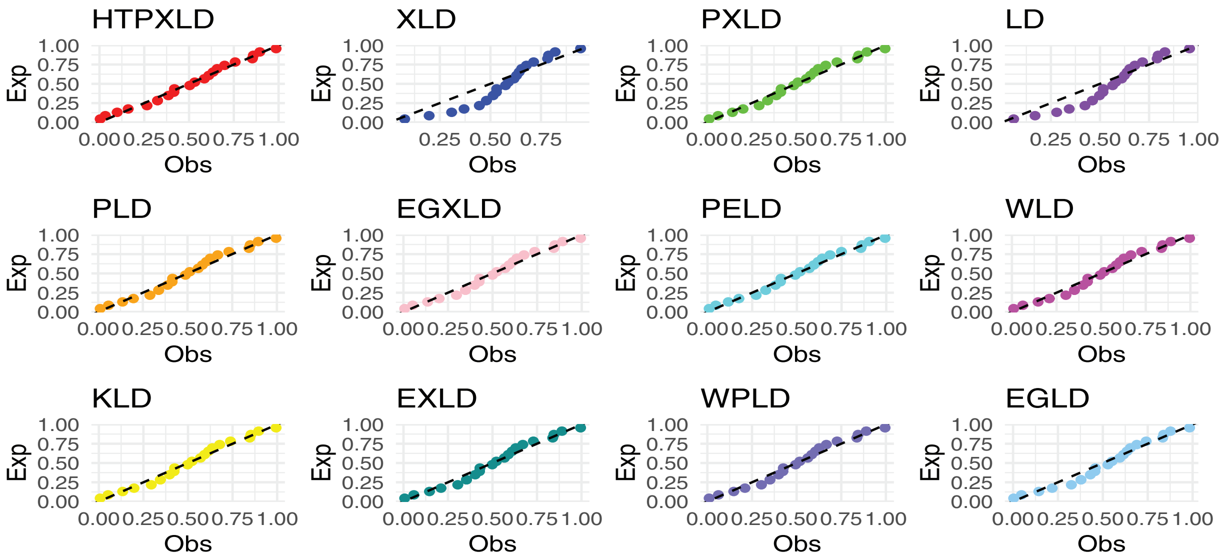

Figure 14: PP plots of competing models for the third dataset

Table 19: The actuarial metrics VaR, TVaR, and TV values for the data set3

Measure	q	HTPXLD	PXLD	PLD	EGXLD	WLD	KLD	EXLD	WPLD
VaR	0.900	5.2743	5.2588	5.2483	5.2616	5.2122	5.2467	5.2178	5.2137
	0.910	5.4370	5.3808	5.3728	5.4142	5.4309	5.3773	5.4270	5.4200
	0.920	5.6196	5.5143	5.5093	5.5600	5.5772	5.5209	5.5884	5.5781
	0.930	5.8273	5.6624	5.6609	5.7224	5.7304	5.6811	5.7451	5.7310
	0.940	6.0675	5.8292	5.8320	5.9065	5.9029	5.8628	5.9216	5.9030
	0.950	6.3520	6.0213	6.0296	6.1198	6.1011	6.0735	6.1248	6.1007
	0.960	6.6995	6.2496	6.2648	6.3749	6.3362	6.3260	6.3660	6.3349
	0.970	7.1441	6.5339	6.5588	6.6952	6.6281	6.6437	6.6661	6.6257
	0.975	7.4226	6.7089	6.7400	6.8936	6.8073	6.8411	6.8504	6.8041
	0.980	7.7588	6.9180	6.9572	7.1321	7.0209	7.0788	7.0706	7.0167
	0.985	8.1833	7.1802	7.2301	7.4331	7.2880	7.3796	7.3461	7.2825
	0.990	8.7616	7.5370	7.6026	7.8462	7.6501	7.7943	7.7203	7.6426
	0.995	9.6903	8.1177	8.2115	8.5262	8.2358	8.4818	8.3269	8.2246
	0.999	11.5697	9.3554	9.5193	10.0045	9.4693	10.0013	9.6097	9.4487
TVaR	0.900	6.7833	6.2786	6.2994	6.4212	6.3610	6.3774	6.3940	6.3588
	0.910	6.9421	6.3852	6.4093	6.5406	6.4705	6.4959	6.5065	6.4680
	0.920	7.1191	6.5025	6.5305	6.6724	6.5910	6.6269	6.6302	6.5880
	0.930	7.3187	6.6333	6.6658	6.8200	6.7251	6.7737	6.7680	6.7216
	0.940	7.5479	6.7815	6.8193	6.9878	6.8766	6.9410	6.9243	6.8725
	0.950	7.8164	6.9534	6.9976	7.1834	7.0523	7.1362	7.1049	7.0473
	0.960	8.1406	7.1587	7.2111	7.4185	7.2616	7.3713	7.3207	7.2557
	0.970	8.5503	7.4164	7.4794	7.7153	7.5233	7.6690	7.5910	7.5160
	0.975	8.8045	7.5757	7.6461	7.9000	7.6850	7.8550	7.7580	7.6768

(Continued)

Table 19 (continued)

Measure	q	HTPXLD	PXLD	PLD	EGXLD	WLD	KLD	EXLD	WPLD
	0.980	9.1094	7.7671	7.8463	8.1228	7.8786	8.0798	7.9583	7.8692
	0.985	9.4919	8.0082	8.0992	8.4050	8.1218	8.3655	8.2102	8.1109
	0.990	10.0103	8.3386	8.4464	8.7939	8.4537	8.7613	8.5544	8.4406
	0.995	10.8416	8.8802	9.0179	9.4386	8.9948	9.4218	9.1167	8.9777
	0.999	12.5396	10.0487	10.2591	10.8520	10.1491	10.8963	10.3206	10.1219
TV	0.900	2.0173	0.8444	0.9123	1.1044	0.8768	1.1089	0.9315	0.8684
	0.910	1.9890	0.8244	0.8925	1.0844	0.8539	1.0917	0.9082	0.8454
	0.920	1.9555	0.8033	0.8718	1.0633	0.8299	1.0736	0.8839	0.8214
	0.930	1.9158	0.7810	0.8497	1.0407	0.8044	1.0543	0.8580	0.7958
	0.940	1.8662	0.7570	0.8258	1.0174	0.7781	1.0339	0.8287	0.7694
	0.950	1.8055	0.7302	0.7993	0.9894	0.7469	1.0109	0.7991	0.7381
	0.960	1.7289	0.7014	0.7704	0.9587	0.7131	0.9857	0.7644	0.7043
	0.970	1.6284	0.6662	0.7383	0.9237	0.6751	0.9574	0.7250	0.6663
	0.975	1.5653	0.6481	0.7171	0.9031	0.6524	0.9406	0.7021	0.6435
	0.980	1.4892	0.6262	0.6950	0.8796	0.6273	0.9220	0.6762	0.6184
	0.985	1.3955	0.6009	0.6692	0.8515	0.5981	0.9001	0.6457	0.5892
	0.990	1.2730	0.5679	0.6359	0.8201	0.5606	0.8733	0.6069	0.5517
	0.995	1.0936	0.5217	0.5878	0.7634	0.5085	0.8366	0.5515	0.4984
	0.999	0.8038	0.4417	0.5042	0.6734	0.4162	0.7755	0.4528	0.4077

Table 20: The actuarial metrics TVP values for the data set3

κ	q	HTPXLD	PXLD	PLD	EGXLD	WLD	KLD	EXLD	WPLD
0.50	0.900	7.7920	6.7008	6.7555	6.9734	6.7994	6.9319	6.8597	6.7930
	0.910	7.9366	6.7974	6.8556	7.0828	6.8975	7.0418	6.9606	6.8908
	0.920	8.0968	6.9042	6.9664	7.2041	7.0060	7.1637	7.0721	6.9987
	0.930	8.2766	7.0238	7.0906	7.3403	7.1273	7.3008	7.1970	7.1195
	0.940	8.4810	7.1600	7.2322	7.4964	7.2657	7.4579	7.3386	7.2572
	0.950	8.7191	7.3184	7.3972	7.6781	7.4257	7.6416	7.5044	7.4164
	0.960	9.0051	7.5094	7.5963	7.8979	7.6182	7.8642	7.7029	7.6078
	0.970	9.3645	7.7495	7.8485	8.1771	7.8609	8.1478	7.9535	7.8492
	0.975	9.5871	7.8998	8.0046	8.3515	8.0112	8.3253	8.1091	7.9985
	0.980	9.8540	8.0802	8.1939	8.5626	8.1923	8.5407	8.2964	8.1784
	0.985	10.1896	8.3087	8.4338	8.8308	8.4209	8.8156	8.5330	8.4055
	0.990	10.6468	8.6226	8.7643	9.2040	8.7340	9.1980	8.8578	8.7165
	0.995	11.3883	9.1411	9.3118	9.8203	9.2490	9.8402	9.3924	9.2270
	0.999	12.9415	10.2696	10.5112	11.1887	10.3572	11.2841	10.5470	10.3258
0.75	0.900	8.2963	6.9119	6.9836	7.2495	7.0186	7.2091	7.0926	7.0101
	0.910	8.4339	7.0035	7.0787	7.3539	7.1110	7.3147	7.1876	7.1021
	0.920	8.5857	7.1050	7.1843	7.4699	7.2135	7.4321	7.2931	7.2041

(Continued)

Table 20 (continued)

κ	q	HTPXLD	PXLD	PLD	EGXLD	WLD	KLD	EXLD	WPLD
	0.930	8.7556	7.2191	7.3030	7.6005	7.3284	7.5644	7.4115	7.3184
	0.940	8.9475	7.3493	7.4387	7.7508	7.4602	7.7164	7.5458	7.4496
	0.950	9.1705	7.5010	7.5971	7.9255	7.6125	7.8944	7.7042	7.6009
	0.960	9.4373	7.6847	7.7889	8.1376	7.7965	8.1106	7.8940	7.7839
	0.970	9.7716	7.9161	8.0331	8.4081	8.0297	8.3871	8.1347	8.0157
	0.975	9.9785	8.0618	8.1839	8.5773	8.1743	8.5604	8.2846	8.1594
	0.980	10.2263	8.2367	8.3676	8.7824	8.3491	8.7712	8.4654	8.3330
	0.985	10.5385	8.4589	8.6011	9.0436	8.5704	9.0406	8.6945	8.5529
	0.990	10.9651	8.7645	8.9233	9.4090	8.8742	9.4163	9.0096	8.8544
	0.995	11.6617	9.2715	9.4587	10.0111	9.3761	10.0493	9.5302	9.3516
	0.999	13.1425	10.3800	10.6372	11.3571	10.4613	11.4780	10.6602	10.4277
0.90	0.900	8.5989	7.0385	7.1204	7.4151	7.1501	7.3755	7.2324	7.1404
	0.910	8.7323	7.1271	7.2126	7.5165	7.2391	7.4785	7.3239	7.2289
	0.920	8.8790	7.2255	7.3151	7.6294	7.3379	7.5931	7.4257	7.3273
	0.930	9.0429	7.3362	7.4305	7.7566	7.4490	7.7225	7.5402	7.4378
	0.940	9.2275	7.4628	7.5626	7.9034	7.5769	7.8714	7.6701	7.5650
	0.950	9.4413	7.6105	7.7170	8.0739	7.7245	8.0460	7.8241	7.7117
	0.960	9.6966	7.7899	7.9045	8.2814	7.9034	8.2584	8.0087	7.8895
	0.970	10.0158	8.0160	8.1439	8.5466	8.1310	8.5308	8.2435	8.1157
	0.975	10.2132	8.1590	8.2915	8.7128	8.2722	8.7015	8.3899	8.2559
	0.980	10.4496	8.3307	8.4719	8.9144	8.4432	8.9095	8.5668	8.4258
	0.985	10.7478	8.5491	8.7014	9.1714	8.6601	9.1756	8.7913	8.6412
	0.990	11.1560	8.8497	9.0187	9.5320	8.9583	9.5473	9.1006	8.9371
	0.995	11.8258	9.3498	9.5469	10.1256	9.4524	10.1748	9.6130	9.4263
	0.999	13.2630	10.4462	10.7128	11.4581	10.5237	11.5943	10.7282	10.4889

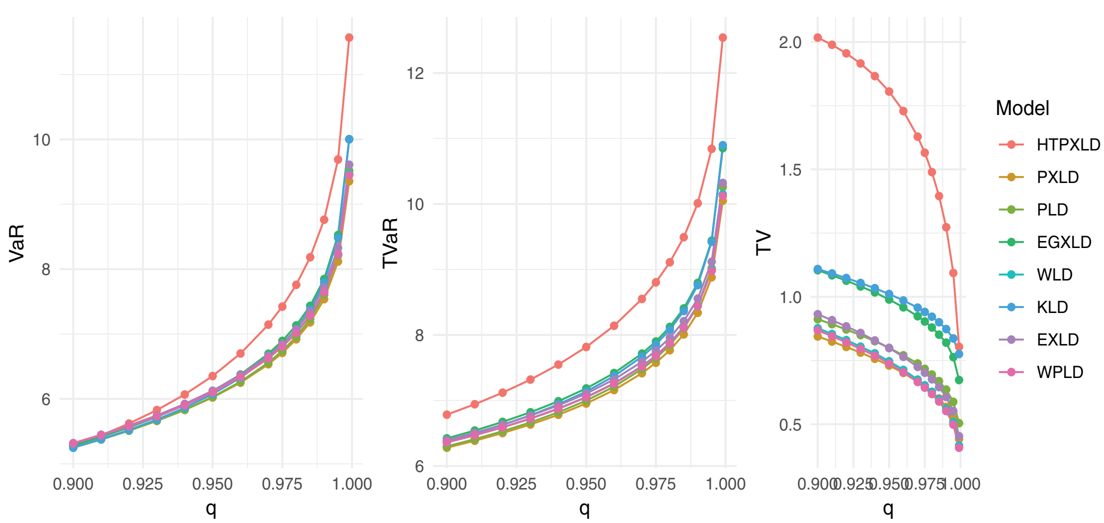

Figure 15: Competing model VaR, TVaR, and TV plots for the third dataset

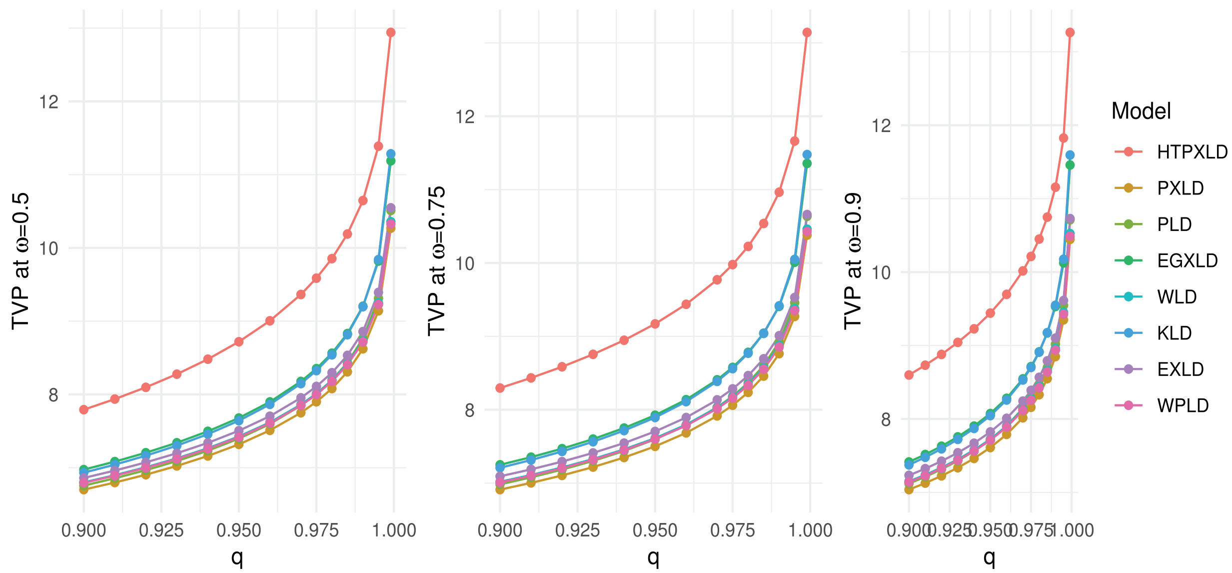

Figure 16: Competing model TVP plots for the third dataset

8 Conclusion

In the applied sciences, modeling heavy-tailed datasets is an important task, especially in domains like finance, medicine, and actuarial analysis. This paper constructs a novel heavy-tailed distribution by combining the PXLD with a heavy-tailed family. Especially when modeling leptokurtic lifespan data, that is, data with thicker tails this novel distribution presents a strongly modified version of the PXLD. With asymmetric forms and different degrees of peakedness, our suggested density gives more versatility, and its hazard rate function has various shapes. We delve into its statistical properties, deriving the quantile function, moments, incomplete moments, stochastic ordering, SS reliability parameter, and some extropy measures. We employ the ML procedure to estimate the model parameters. To assess the effectiveness of our proposed estimators, we conduct various simulation experiments. These experiments will evaluate the estimator's performance using metrics like an average estimate, relative bias, bias, mean squared error, root mean squared error, average interval length, and coverage probability. We employ our suggested model to examine three real-world datasets to demonstrate its usefulness. The simulation analysis provided evidence that MLEs exhibit improved accuracy with increasing sample size. This is supported by the observed decrease in MSE, which is consistent with the theoretical expectation of parameter estimates converging toward their true values as the sample size grows. As sample numbers rise, the CP of the approximate CIs improves. As a result, we can be more certain that the actual parameter values fall inside the stated confidence intervals. Next, we evaluate its effectiveness in comparison to well-known rival models, emphasizing its benefits. A limitation of this study lies in its exclusive reliance on deriving point and interval estimates using the maximum likelihood method in the case of a complete sample. The simulation analysis presented in this work focuses specifically on scenarios with large sample sizes. Future studies should examine how well the HTPXLD performs in more realistic settings, such as those requiring ranked set sampling. Future studies should examine the HTPXLD's performance on a larger variety of datasets with a range of attributes to fully evaluate its adaptability.

Acknowledgement: The authors thank King Saud University, Riyadh, Saudi Arabia for Supporting this research by Project Number (RSPD2025R548).

Funding Statement: This research is supported by researchers Supporting Project Number (RSPD2025R548), King Saud University, Riyadh, Saudi Arabia.

Author Contributions: Mohammed Elgarhy: Writing—original draft, Validation, Methodology, Formal analysis, Conceptualization, Writing—review, Investigation. Amal S. Hassan: Writing—original draft, Validation, Methodology, Formal analysis, Conceptualization, Writing—review, Investigation. Najwan Alsadat: Writing—original draft, Validation, Methodology, Formal analysis, Conceptualization, Writing—review, Investigation. Oluwafemi Samson Balogun: Writing—original draft, Validation, Methodology, Formal analysis, Conceptualization, Writing—review, Investigation. Ahmed W. Shawki: Writing—original draft, Validation, Methodology, Formal analysis, Conceptualization, Writing—review, Investigation. Ibrahim E. Ragab: Writing—original draft, Validation, Methodology, Formal analysis, Conceptualization, Writing—review, Investigation. All authors reviewed the results and approved the final version of the manuscript.

Availability of Data and Materials: All data generated or analyzed during this study are included in this published article.

Ethics Approval: Not applicable.

Conflicts of Interest: The authors declare no conflicts of interest to report regarding the present study.

References

1. Chouia S, Zeghdoudi H. The XLindley distribution: properties and application. J Stat Theory Appl. 2021;20(2):318–27. doi:10.2991/jsta.d.210607.001.
2. Krishnarani S. On a power transformation of half-logistic distribution. J Probab Stat. 2016;2016(5):2084236. doi:10.1155/2016/2084236.
3. Al-Omari A, Alhyasat K, Ibrahim K, Abu Bakar M. Power length-biased Suja distribution: properties and application. Electron J Appl Stat Anal. 2019;12(12):429–52. doi:10.1285/i20705948v12n2p429.
4. Hassan AS, Nassar SG. Power lindley-G family. Ann Data Sci. 2019;6(2):189–210. doi:10.1007/s40745-018-0159-y.
5. Shanker R, Shukla KK. Power weighted Sujayha distribution with properties and application to survival times of patients of head and neck cancer. Reliab Theory Appl. 2023;18(3):568–81.
6. Rady E, Hassanein W, Elhaddad T. The power Lomax distribution with an application to bladder cancer data. SpringerPlus. 2016;5:1–22. doi:10.1186/s40064-016-3464-y.
7. Hassan AS, Nassr SG. Power lomax poisson distribution: properties and estimation. J Data Sci. 2018;16(1):105–28. doi:10.6339/JDS.201801_16(1).0007.
8. Afify AZ, Gemeay AM, Alfaer NM, Cordeiro GM, Hafez EH. Power-modified kies-exponential distribution: properties, classical and bayesian inference with an application to engineering data. Entropy. 2022;24(7):883. doi:10.3390/e24070883.
9. Hassan AS, Assar SM, Abd Elghaffar AM. Statistical properties and estimation of power-transmuted inverse Rayleigh distribution. Stat Trans New Series. 2020;21(3):1–20. doi:10.21307/stattrans-2020-046.
10. Meriem B, Gemeay AM, Almetwally EM, Halim Z, Alshawarbeh E, Abdulrahman AT, et al. The power XLindley distribution: statistical inference, fuzzy reliability, and COVID-19 application. J Funct Spaces. 2022;2022(2):9094078. doi:10.1155/2022/9094078.
11. Marshall AW, Olkin I. A new method for adding a parameter to a family of distributions with application to the exponential and Weibull families. Biometrika. 1997;84(3):641–52. doi:10.1093/biomet/84.3.641.
12. Eugene N, Lee C, Famoye F. Beta-normal distribution and its applications. Commun Stat-Theor Meth. 2002;31(4):497–512. doi:10.1081/STA-120003130.
13. Cordeiro GM, de Castro M. A new family of generalized distributions. J Stat Comput Simul. 2011;81(7):883–98. doi:10.1080/00949650903530745.
14. Alzaatreh A, Lee C, Famoye F. A new method for generating families of continuous distributions. METRON. 2013;71(1):63–79. doi:10.1007/s40300-013-0007-y.

15. Bourguignon M, Silva RB, Cordeiro GM. The Weibull-G family of probability distributions. J Data Sci. 2014;12(1):53–68. doi:10.6339/JDS.201401_12(1).0004.
16. Kumar D, Singh U, Singh SK. A method of proposing new distribution and its application to bladder cancer patient data. J Stat Probab Lett. 2015;2:235–45.
17. Cordeiro GM, Alizadeh M, Diniz Marinho PR. The type I half-logistic family of distributions. J Stat Comput Simul. 2015;86(4):707–28. doi:10.1080/00949655.2015.1031233.
18. Cordeiro GM, Alizadeh M, Ortega EMM. The exponentiated half-logistic family of distributions: properties and applications. J Probab Stat. 2014;2014(1):864396. doi:10.1155/2014/864396.
19. Bodhisuwan W, Sangsanit Y. The Topp-Leone generator of distributions: properties and inferences. Songklanakarin J Sci Technol. 2016;38(5):537–48.
20. Alizadeh M, Cordeiro GM, Pinho LGB, Ghosh I. The Gompertz-G family of distributions. J Stat Theory Pract. 2016;11(1):179–207. doi:10.1080/15598608.2016.1267668.
21. Chipepa F, Oluyede B, Makubate B, Fagbamigbe AF. The beta odd Lindley-G family of distributions with applications. J Probab Stat Sci. 2019;17(1):51–83.
22. Hassan AS, Sabry MAH, Elsehery AM. A new probability distribution family arising from truncated power lomax distribution with application to weibull model. Pak J Stat Oper Res. 2020;16(4):661–74. doi:10.18187/pjsor.v16i4.3442.
23. Kavya P, Manoharan M. Some parsimonious models for lifetimes and applications. J Stat Comput Simul. 2021;91:3693–708. doi:10.1080/00949655.2021.1946064.
24. Hassan AS, Al-Omari AI, Hassan RR, Alomani G. The odd inverted Topp Leone H family of distributions: estimation and applications. J Radiat Res Appl Sci. 2022;15(3):365–79. doi:10.1016/j.jrras.2022.08.006.
25. Korkmaz MÇ., Cordeiro GM, Yousof HM, Pescim RR, Afify AZ, Nadarajah S. The Weibull Marshall-Olkin family: regression model and application to censored data. Commun Stat-Theor Meth. 2018;48(16):4171–94. doi:10.1080/03610926.2018.1490430.
26. Souza L, de Oliveira WR, de Brito CCR, Chesneau C, Fernandes R, Ferreira TAE. Sec-G class of distributions: properties and applications. Symmetry. 2022;14(2):299. doi:10.3390/sym14020299.
27. Hassan AS, Alsadat N, Chesneau C, Shawki AW. A novel weighted family of probability distributions with applications to world natural gas, oil, and gold reserves. Mathem Biosci Eng. 2023;20(11):19871–911. doi:10.3934/mbe.2023880.
28. Shah Z, Khan DM, Khan Z, Faiz N, Hussain S, Anwar A, et al. A new generalized logarithmic-X family of distributions with biomedical data analysis. Appl Sci. 2023;13(6):3668. doi:10.3390/app13063668.
29. Musekwa RR, Gabaitiri L, Makubate B. A new technique to generate families of continuous distributions. Revista Colombiana De Estadistica. 2024;47(2):329–54. doi:10.15446/rce.v47n2.112245.
30. Makubate B, Chipepa F, Oluyede B, Moagi G. The Marshall-Olkin-exponentiated half logistic-G family of distributions: model, properties and applications. J Statist Manag Syst. 2024;27(7):1243–59. doi:10.47974/JSMS-854.
31. Ahmad Z, Mahmoudi E, Hamedani CG, Kharazmi O. New methods to define heavy-tailed distributions with applications to insurance data. J Taibah Univ Sci. 2020;14(1):359–82. doi:10.1080/16583655.2020.1741942.
32. Ahmad Z, Mahmoudi E, Hamedani GG. A class of claim distributions: properties, characterizations and applications to insurance claim data. Commun Stat-Theor Meth. 2020;51(7):2183–208. doi:10.1080/03610926.2020.1772306.
33. Nadarajah S, Lyu J. New discrete heavy tailed distributions as models for insurance data. PLoS One. 2025;18(5):e0285183. doi:10.1371/journal.pone.0285183.
34. Nair J, Wierman A, Zwart B. The fundamentals of heavy tails: properties, emergence, and estimation. Cambridge, UK: Cambridge University Press; 2022. doi:10.1017/9781009053730.
35. McNeil AJ. Estimating the tails of loss severity distributions using extreme value theory. ASTIN Bull. 1997;27(1):117–37. doi:10.2143/AST.27.1.563210.
36. Olmos NM, Gomez-Deniz E, Venegas O. The heavy-tailed gleser model: properties, estimation, and applications. Mathematics. 2022;10(23):4577. doi:10.3390/math10234577.

37. Zhao W, Khosa SK, Ahmad Z, Aslam M, Affy AZ. Type-I heavy tailed family with applications in medicine, engineering and insurance. PLoS One. 2020;15(8):e0237462. doi:10.1371/journal.pone.0237462.
38. Moakofi T, Oluyede B. The type I heavy-tailed odd power generalized Weibull-G family of distributions with applications. Commun Fac Sci Univ Ankara Series A1 Math Stat. 2023;72(4):921–58. doi:10.31801/cfsuasmas.1195058.
39. Moakofi T, Oluyede B, Tlhaloganyang B, Puoetsile A. A new family of heavy-tailed generalized Topp-Leone-G distributions with applications. Pak J Stat Oper Res. 2024;20(2):233–60. doi:10.18187/pjsor.v20i2.4458.
40. Ahmad Z, Mahmoudi E, Dey S. A new family of heavy tailed distributions with an application to the heavy tailed insurance loss data. Commun Statist-Simulat Computat. 2020;51(8):4372–95. doi:10.1080/03610918.2020.1741623.
41. Corless RM, Gonnet GH, Hare DE, Jeffrey DJ, Knuth DE. On the Lambert W function. Adv Comput Math. 1995;5(1):329–59. doi:10.1007/BF02124750.
42. Kenney JF, Keeping E. Mathematics of statistics (part one). Louisville, KY, USA: D. Van Nostrand Company, Inc.; 1962.
43. Moors JJA. A quantile alternative for kurtosis. J Royal Stat Soc: Series D (Stat). 1988;37(1):25–32.
44. Butler RJ, McDonald JB. Using incomplete moments to measure inequality. J Econom. 1989;42(1):109–19. doi:10.1016/0304-4076(89)90079-1.
45. Shaked M, Shanthikumar JG. Stochastic orders and their applications. New York, NY, USA: Academic Press; 1994.
46. Shannon CE. A mathematical theory of communication. Bell Syst Tech J. 1948;27(3):379–423. doi:10.1002/j.1538-7305.1948.tb01338.x.
47. Lad F, Sanfilippo G, Agr G. Extropy: complementary dual of entropy. Statist Sci. 2015;30(1):40–58. doi:10.1214/14-STS430.
48. Balakrishnan N, Buono F, Longobardi M. On weighted extropies. Commun Stat-Theor Meth. 2022;51(18):6250–67. doi:10.1080/03610926.2020.1860222.
49. Artzner P. Application of coherent risk measures to capital requirements in insurance. N Am Actuar J. 1999;3(2):11–25. doi:10.1080/10920277.1999.10595795.
50. Landsman Z. On the tail mean-variance optimal portfolio selection. Insur Math Econ. 2010;46(3):547–53. doi:10.1016/j.insmatheco.2010.02.001.
51. Lindley DV. Fiducial distributions and Bayes' theorem. J Royal Stat Soc: Series B (Meth). 1958;20(1):102–10. doi:10.1111/j.2517-6161.1958.tb00278.x.
52. Musekwa RR, Makubate B. A flexible generalized XLindley distribution with application to engineering. Sci Afr. 2024;24(2):e02192. doi:10.1016/j.sciaf.2024.e02192.
53. Rajitha CS, Akhilnath A. Generalization of the Lindley distribution with application to COVID-19 data. Int J Data Sci Anal. 2022;23:1–21. doi:10.1007/s41060-022-00369-2.
54. Abdelmoezz S, Mohamed SM. The kumaraswamy lindley regression model with application on the Egyptian stock exchange: numerical study, regression model. Jurnal Matematika, Statistika Dan Komputasi. 2021;18(1):1–11. doi:10.20956/j.v18i1.14784.
55. MirMostafaee SMTK, Alizadeh M, Altun E, Nadarajah S. The exponentiated generalized power Lindley distribution: properties and applications. Appl Mathem-J Chin Univ. 2019;34(2):127–48. doi:10.1007/s11766-019-3515-6.
56. Ghitany ME, Al-Mutairi DK, Balakrishnan N, Al-Enezi LJ. Power Lindley distribution and associated inference. Computat Statist Data Analy. 2013;64(9):20–33. doi:10.1016/j.csda.2013.02.026.
57. Asgharzadeh AKBAR, Nadarajah S, Sharafi F. Weibull Lindley distribution. Revstat-Statist J. 2018;16(1):87–113. doi:10.57805/revstat.v16i1.234.
58. Bakouch HS, Al-Zahrani BM, Al-Shomrani AA, Marchi VA, Louzada F. An extended Lindley distribution. J Korean Statist Soc. 2012;41(1):75–85. doi:10.1016/j.jkss.2011.06.002.

59. Lemonte AJ, Barreto-Souza W, Cordeiro GM. The exponentiated Kumaraswamy distribution and its log-transform. Braz J Probab Stat. 2013;27(1):31–53. doi:10.1214/11-BJPS149.
60. Lee ET, Wang J. Statistical methods for survival data analysis. New York, NY, USA: John Wiley & Sons; 2003. Vol. 476.